PHYSICAL REVIEW D VOLUME 47, NUMBER 2 15 JANUARY 1993

Neutralino relic density in minimal $N=1$ supergravity

Manuel Drees
Theorie-Gruppe, DESY, Notkestrasse 85, D2000 Hamburg 52, Germany

Mihoko M. Nojiri*
Theory Group, Stanford Linear Accelerator Center, P.O. Box 4349, Stanford, California 94305
(Received 17 July 1992)

We compute the cosmic relic (dark-matter) density of the lightest supersymmetric particle (LSP) in the framework of minimal $N=1$ supergravity models with radiative breaking of the electroweak gauge symmetry. To this end, we recalculate the cross sections for all possible annihilation processes for a general, mixed neutralino state with arbitrary mass. Our analysis includes effects of all Yukawa couplings of third-generation fermions, and allows for a fairly general set of soft supersymmetry- (SUSY-) breaking parameters at the Planck scale. We find that a cosmologically interesting relic density emerges naturally over wide regions of parameter space. However, the requirement that relic neutralinos do not overclose the Universe does not lead to upper bounds on SUSY-breaking parameters that are strictly valid for all combinations of parameters and of interest for existing or planned collider experiments; in particular, gluino and squark masses in excess of 5 TeV cannot strictly be excluded. On the other hand, in the "generic" case of a gauginolike neutralino whose annihilation cross sections are not "accidentally" enhanced by a nearby Higgs boson or Z pole, all sparticles should lie within the reach of the proposed pp and e^+e^- supercolliders. We also find that requiring the LSP to provide all dark matter predicted by inflationary models imposes a strict lower bound of 40 GeV on the common scalar mass m at the Planck scale, while the lightest sleptons would have to be heavier than 100 GeV. Fortunately, a large relic neutralino density does not exclude the possibility that charginos, neutralinos, gluinos, and squarks are all within the reach of the CERN e^+e^- collider LEP 200 and the Fermilab Tevatron.

PACS number(s): 95.30.Cq, 11.30.Pb, 12.15.Ji, 14.80.Ly

I. INTRODUCTION

It is by now well established [1] that the observed, luminous matter in the Universe cannot account for its total mass. Cosmological mass densities are usually expressed as the ratio $\Omega \equiv \rho/\rho_c$, where $\rho_c \simeq 2\times 10^{-29} h^2$ g/cm^3 is the "critical" mass density that yields a flat universe, as favored by inflationary cosmology [2]; $\rho < (>)\rho_c$ corresponds to an open (closed) universe, i.e., a metric with negative (positive) curvature. The dimensionless parameter h is proportional to the Hubble "constant" H describing the expansion of the Universe: $H \equiv 100h$ km/sec Mpc. Observations yield $0.5 \le h \le 1$. Even if one broadly defines luminous matter as everything that emits any kind of electromagnetic radiation, when averaged over the volume of the (visible) Universe it cannot give $\Omega > 0.01$. In contrast, from the observed orbits of hydrogen clouds around a variety of galaxies, including our own, one derives [1] $\Omega \ge 0.1$; and from the motion of (clusters of) galaxies within superclusters one can deduce [1] $\Omega \ge 0.3$–0.4. Finally, as indicated above, $\Omega = 1$ is predicted [2] by models of inflationary cosmology; such models are currently favored, since they can solve other cosmological problems, e.g., the flatness, horizon, and magnetic monopole problems.

The nature of the missing or dark matter (DM) cannot be derived directly from present observations. However, within standard (big bang) cosmology, the observed abundances of light elements (D, He, Li) can only be understood [3] if the total baryonic mass density is less than about $0.1\rho_c$. The discrepancy between the lower bound on the total mass density and the upper bound on the baryonic one has led to speculations [4] that some neutral, weakly interacting stable particle might provide the bulk of the mass density today. In particular, it was observed almost 10 years ago [5] that the lightest supersymmetric (SUSY) particle (LSP) is a good candidate for dark matter. Its stability is guaranteed by a discrete symmetry called R parity, which can be imposed in most phenomenologically viable SUSY models; in particular, R parity is automatically conserved in the simplest realistic SUSY model [6,7], the minimal supersymmetric standard model (MSSM). This explanation is especially attractive since the primary motivation for SUSY has nothing to do with the DM problem; rather, SUSY *automatically* provides a DM candidate "for free." Moreover, for "natural" choices of parameters (to be specified below), Ω turns out to be [5] of approximately the right order of magnitude.

The primary motivation for the introduction of supersymmetry stems from the observation [8] that in SUSY models large hierarchies between mass scales are automatically protected against (quadratically divergent) radiative corrections, in contrast [9] with nonsupersymmetric models. In particular, within the nonsupersymmetric standard model (SM) it is extremely unnatural to

*Electronic address: kekvax::nojirin,nojirim@slacvm

assume the scale of electroweak symmetry breaking, characterized by the vacuum expectation value (VEV) of the Higgs field $\langle H \rangle = 175$ GeV, to be much smaller than the scale of grand unification $M_X \simeq 10^{15}-10^{16}$ GeV or the Planck scale $M_P \simeq 10^{19}$ GeV. On the other hand, in the MSSM radiative corrections are under control, provided only that the mass scale of the superpartners is not much bigger than 1 TeV. The relation between the scale of electroweak symmetry breaking and sparticle masses is even more direct in minimal supergravity (SUGRA) models where the breakdown of electroweak gauge symmetry is induced by (logarithmic) radiative corrections to the parameters of the Higgs potential [10,7]. These models also have the practical advantage that they allow to describe the whole spectrum of superparticles (sparticles) in terms of a small number of free parameters. Moreover, the resulting sparticle spectra almost automatically satisfy constraints from K and B physics [11], and lead to small additional contributions to electroweak observables [12], in agreement with results from the CERN e^+e^- collider LEP [13]. Finally, precision measurements at LEP have shown [14] that the nonsupersymmetric SM does not lead to a grand unification of the gauge couplings, whereas in the MSSM all three gauge couplings meet at scale $M_X \simeq 10^{16}$ GeV. While this result does not depend [15,16] on the constraints on the sparticle spectrum imposed by minimal SUGRA, it does lend credence to the assumption that there is no additional threshold between the weak scale and M_X; this assumption is an important ingredient of SUGRA models with radiative symmetry breaking.

Quite a few papers have already been published in the last decade that contain calculations of the relic LSP density in some version of the MSSM. However, older papers [5,17] often assume rather light sparticles, in conflict with recent experimental bounds. Moreover, many previous calculations [5,17–20] involved simplifying assumptions about the sparticle spectrum, which were often in conflict with SUGRA predictions (e.g., by assuming the LSP to have the same mass as quarks). Some computations [21–24] do take the SUGRA relations between sfermion and gaugino masses into account, but the additional constraints on model parameters imposed by radiative gauge symmetry breaking have still been ignored in these papers. Moreover, in Refs. [21–24] only the case of a "light" LSP, with mass below that of the W boson, has been treated. Indeed, only two calculations of the annihilations cross sections of a heavy LSP exist to date [18,19], and neither of them is fully complete. In Ref. [18] the annihilation into one Higgs boson and one gauge boson has not been included; moreover, the given expressions do not seem to be applicable if the mass of the LSP is less than half the mass of the heaviest Higgs boson. Reference [19] does treat the full list of possible final states, but only considers unmixed (pure) neutralino states; we will see that this actually gives wrong results for the gauginolike LSP even in the limit of infinite LSP mass. The results of Ref. [19] have been used in Refs. [20,23,25] as well. We have independently computed *all* relevant annihilation cross sections for a *general,* mixed LSP eigenstate. This part of our work should be useful beyond the context of the more restrictive SUGRA models. Very recently another calculation of the relic density of heavy LSP's has appeared [26]. The authors state that they generalized the results of Ref. [19] by including neutralino mixing, but no explicit expressions are given; moreover, no SUGRA mass relations are assumed.

We are aware of only two calculations of relic LSP densities [27,25] in which the constraints imposed by radiative gauge symmetry breaking have been taken into account. However, in these papers a specific SUSY-breaking scheme, the "no-scale" ansatz [28], has been assumed; in this scheme the LSP density turned out to be too low to account for all dark matter.[1] Moreover, the Higgs sector has only been treated in the tree-level approximation. The importance of Higgs-boson-exchange contributions has been pointed out in Ref. [29], again using tree-level formula for Higgs boson masses. However, radiative corrections to these masses can be [30] substantial if the top quark is heavy, $m_t > 100$ GeV, which now seems likely.[2]

In this paper we compute the LSP relic density in minimal SUGRA models with radiative gauge symmetry breaking. We use three free parameters to describe the SUSY breaking, as opposed to only one in Refs. [27,25]. Because of the constraints imposed by radiative gauge symmetry breaking, which in particular fix the Higgs spectrum for a given set of SUSY breaking parameters and given m_t, the resulting parameter space is still sufficiently small to allow for an exhaustive scan; we thus do not have to rely on "simplifying assumptions" of often dubious validity. As indicated above, we always include neutralino mixing, as well as *all* kinematically accessible final states, when computing the LSP annihilation cross section. Our analysis of radiative symmetry breaking includes effects of the Yukawa couplings of the b quark and τ lepton, which can be quite important [31,32]. Mixing between the superpartners of left- and right-handed fermions is also treated exactly. One-loop corrections to the Higgs sector are included, and all experimental constraints on sparticle masses are taken into account.

We find that the model can easily yield sufficient dark matter to close the Universe, *if* the SUSY-breaking common scalar mass m at scale M_X exceeds 40 GeV. This conclusion is closely related to the result of Refs. [33,34] that a single light sfermion suffices to make the relic density of a gauginolike LSP uninterestingly small. A qualitatively similar result has been found in Ref. [24] in a more general context. On the other hand, requiring the LSP not to overclose the Universe does *not* lead to upper bounds on sparticle masses which are both relevant for existing or planned experiments and are valid for the en-

[1]This result can also be derived from Refs. [22,23] once one makes use of the fact that these models cannot support a Higgsino-like LSP; see also Ref. [24].

[2]Leading one-loop corrections to the Higgs sector are included in Ref. [24], but only for light LSP's, and without the constraints imposed by radiative gauge symmetry breaking.

tire parameter space. Of course, it is quite unnatural [35,16] to assume sparticles to be much heavier than the W and Z bosons, but naturalness arguments cannot be translated into strict upper bounds; even a rather high [18,19] bound from cosmology would therefore have been welcome. Alas, there are two different ways in which such a bound can be circumvented. One possibility is to have a light Higgsino-like LSP, with all SUSY-breaking masses being very large. Note that the Higgsino mass does *not* break supersymmetry; moreover, we argue that in such a scenario, supersymmetry would be extremely difficult to discover in laboratory experiments. The constraints from radiative gauge symmetry breaking exclude the possibility to have a Higgsino-like LSP if the top quark is heavy, the precise bound on m_t depending on the ratios of the soft SUSY breaking parameters. The second possibility to allow for a very heavy sparticle spectrum is to choose the LSP mass to be close to half the mass of the pseudoscalar Higgs boson; this strongly enhances the annihilation of the LSP into SM fermions, in particular, b quarks and τ leptons. Within the framework of minimal SUGRA, this scenario necessitates a large ratio $\tan\beta$ of the VEV's of the two Higgs fields of the model, but such solutions can be realized quite easily [31,32].

The remainder of this paper is organized as follows. In Sec. II we briefly describe the formalism necessary to compute the DM density for a given LSP annihilation cross section. We also list all possible LSP annihilation processes, and give a short description of the parameter space of minimal SUGRA models. In Sec. III we present illustrative examples of LSP densities in such models. The effects of s-channel poles as well as thresholds, where new annihilation channels open up, are discussed. We also explicitly demonstrate the importance of the SUGRA imposed running of sfermion and Higgs-boson masses. Finally, we study the dependence of the DM density on the free parameters of the model by means of several contour plots. Section IV is devoted to a discussion of the bounds that can be derived from the requirement that the LSP relic density lies in the cosmologically interesting region. As already mentioned above, a strict upper bound on sparticle masses can only be derived if we artificially restrict the parameter space of the model. In contrast, a nontrivial *lower* bound on slepton masses can be derived from the requirement that the LSP relic density be close to the critical density; however, the masses of the gluino, the light chargino, and the squarks can all be near their present lower bounds. Finally, in Sec. V we summarize our results and draw some conclusions. Complete lists of all LSP annihilation matrix elements are given in Appendix A, and Appendix B contains an example of a check of some amplitudes for the production of longitudinal gauge bosons using the equivalence theorem.

II. FORMALISM

In this section we describe the formalism necessary to describe the numerical results of Secs. III and IV. We first (Sec. II A) give a short summary of the calculation of the present day DM density for given mass and annihilation cross section of the dark matter candidate χ. Section II B contains a brief description of the MSSM; it also contains a list of all annihilation channels of our DM candidate. The resulting annihilation cross section will turn out to depend on the *whole* sparticle and Higgs boson spectrum. In Sec. II C we therefore give a brief summary of minimal SUGRA models, where the whole spectrum can be computed in terms of four free parameters.

A. Calculation of the DM density

We begin with a brief description of the calculation of the present relic mass density of a DM candidate χ, assuming that the mass m_χ as well as the annihilation cross section $\sigma_{\rm ann}(\chi\chi\rightarrow\text{anything})$ are known. Following the prescription of Refs. [4,18], we first introduce the freeze-out temperature T_F, below which the $\chi\chi$ reaction rate is (much) smaller than the expansion rate of the Universe. It is convenient to express (inverse) temperatures in terms of the dimensionless quantity $x\equiv m_\chi/T$; the freeze-out temperature can then iteratively be computed from

$$x_F=\ln\frac{0.0764M_P(a+6b/x_F)c(2+c)m_\chi}{\sqrt{g_*x_F}}\ . \tag{1}$$

Here $M_P=1.22\times10^{19}$ GeV is the Planck mass, and a and b are the first two coefficients in the Taylor expansion of the annihilation cross section with respect to the relative velocity v of the $\chi\chi$ pair in its center-of-mass frame:

$$v\sigma_{\rm ann}(\chi\chi\rightarrow\text{anything})=a+bv^2\ ; \tag{2}$$

notice that v is *twice* the velocity of χ in the $\chi\chi$ c.m. system (c.m.s.) frame. Furthermore, g_* is the effective number of relativistic degrees of freedom at $T=T_F$. A highly relativistic boson (fermion) contributes 1 (7/8) to g_*, whereas very nonrelativistic (slow) particles do not contribute at all. However, often T_F turns out to be close to the mass of one of the heavy particles of the SM (the c, b, or t quark, the τ lepton, or the W or Z boson); in this case a careful treatment of the threshold is necessary [4] if ugly jumps in the curves are to be avoided. Finally, the constant c in Eq. (1) is a numerical parameter introduced [4] to achieve smooth matching of approximate solutions of the Boltzmann equation above and below T_F; following Ref. [18] we chose $c=1/2$. Given x_F and $\sigma_{\rm ann}$, one can compute

$$\Omega_\chi h^2\equiv\frac{\rho_\chi}{\rho_c/h^2}=\frac{1.07\times10^9/\text{GeV}\,x_F}{\sqrt{g_*}M_P(a+3b/x_F)}\ , \tag{3}$$

where the rescaled Hubble constant h and the critical density ρ_c have already been introduced in Sec. I.[3]

[3]Within the framework of inflationary cosmology, Eq. (3) should strictly speaking be interpreted as a calculation of the expansion rate, rather than a calculation of the density. After all, inflation predicts [2] $\Omega=1$ to high precision, *independent* of the details of the particle physics model. However, only for a small range of values of the (absolute) mass density ρ does H, and thus the age of the Universe, come out close to the observed value.

Equations (1)–(3) describe a simple, approximate solution of the Boltzmann equation that determines the abundance of any particle species. While not strictly correct [36], in most cases this treatment reproduces the exact numerical solution to 10–20% accuracy [4,18]; given that h^2 in Eq. (3) is only known to a factor of 2, this accuracy is fully sufficient for our purposes. However, it has recently been pointed out [37] that there are three cases in which this approximation fails badly: close to a threshold where a new annihilation channel opens up that dominates the total annihilation cross section; close to a very narrow s-channel resonance; and if the next-to-lightest sparticle χ' is close in mass to the LSP, and $\sigma_{\rm ann}(\chi\chi' \to \text{anything}) \gg \sigma_{\rm ann}(\chi\chi \to \text{anything})$. Unfortunately, in these three cases the proper treatment [37] is considerably more cumbersome than Eqs. (1)–(3). For reasons of computational simplicity we will therefore use the approximate treatment throughout, but we will be careful to point out the situations where it might fail, and will qualitatively describe the result of the proper treatment in such cases.

Note that x_F in Eq. (3) is almost independent of m_χ and $\sigma_{\rm ann}$; we find $15 \leq x_F \leq 30$ for experimentally allowed choices of parameters (see below). The number of degrees of freedom g_* at $T_F \simeq m_\chi/20$ increases monotonically with m_χ, but again the m_χ dependence is quite small: $8 \leq \sqrt{g_*} \leq 10$ for 20 GeV $\leq m_\chi \leq 1$ TeV. The details of the model (particle masses and couplings) affect the prediction for Ω_χ therefore predominantly through the coefficients a and b describing the annihilation cross section; we now briefly describe the calculation of this cross section.

B. The annihilation cross section

Within the MSSM, only the lightest neutralino is left [38] as a viable DM candidate. A stable LSP has to be [39] both electrically and color neutral, since otherwise it would have been found in searches for exotic isotopes. This leaves one with the lightest neutralino and the lightest sneutrino, but the latter is excluded by a combination of the bound on the invisible decay width of the Z boson obtained at LEP [40] and the limits derived from the unsuccessful search for relic sneutrinos using germanium detectors [41].

The sparticle spectrum of the MSSM contains [6,7] four neutralino states: The superpartners of the B and W_3 gauge bosons, and the superpartners of the neutral Higgs bosons H_1^0 and H_2^0 with hypercharge $-\frac{1}{2}$ and $+\frac{1}{2}$, respectively. However, after electroweak gauge symmetry breaking these current eigenstates mix; their mass matrix in the basis $(\tilde{B}, \tilde{W}_3, \tilde{h}_1^0, \tilde{h}_2^0)$ is given by

$$\mathcal{M}^0 = \begin{pmatrix} M_1 & 0 & -M_Z \sin\theta_W \cos\beta & M_Z \sin\theta_W \sin\beta \\ 0 & M_2 & M_Z \cos\theta_W \cos\beta & -M_Z \cos\theta_W \sin\beta \\ -M_Z \sin\theta_W \cos\beta & M_Z \cos\theta_W \cos\beta & 0 & -\mu \\ M_Z \sin\theta_W \sin\beta & -M_Z \cos\theta_W \sin\beta & -\mu & 0 \end{pmatrix}, \tag{4}$$

where we have used the convention of Refs. [6,42], which we will follow throughout. Assuming grand unification of the gauge couplings implies a relation between the SUSY-breaking gaugino masses M_1 and M_2 as well as the gluino mass $m_{\tilde{g}} = |M_3|$:

$$M_1 = \tfrac{5}{3} \tan^2\theta_W M_2 = \frac{5\alpha_{\rm em}}{3\alpha_s \cos^2\theta_W} M_3 , \tag{5}$$

where $\alpha_{\rm em}$ is the electromagnetic coupling constant and α_s is the strong coupling. The angle β in Eq. (4) is defined via $\tan\beta \equiv \langle H_2^0 \rangle / \langle H_1^0 \rangle$. Finally, the parameter μ describes the supersymmetric contribution to the Higgs-boson (Higgsino) masses.

In general the LSP is a complicated mixture [42–44] of the four current eigenstates; in our numerical calculations we take full account of this mixing by diagonalizing the mass matrix (4) numerically. However, in the limit $|M_1| + |\mu| \gg M_Z$ this diagonalization can quite easily be carried out perturbatively. Since this proves helpful for a qualitative understanding of our numerical results, we list the eigenvalues m_i and eigenvectors $\mathbf{e}_i$ of the mass matrix (4), keeping terms up to $O(M_Z)$:

$$m_1 = M_1 ,$$
$$\mathbf{e}_1 = \left[1, 0, \frac{M_Z \sin\theta_W (\cos\beta M_1 + \sin\beta\mu)}{\mu^2 - M_1^2} , \frac{M_Z \sin\theta_W (\sin\beta M_1 + \cos\beta\mu)}{M_1^2 - \mu^2} \right] , \tag{6a}$$

$$m_2 = M_2 ,$$
$$\mathbf{e}_2 = \left[0, 1, \frac{M_Z \cos\theta_W (\cos\beta M_2 + \sin\beta\mu)}{M_2^2 - \mu^2} , \frac{M_Z \cos\theta_W (\sin\beta M_2 + \cos\beta\mu)}{\mu^2 - M_2^2} \right] , \tag{6b}$$

$$m_3 = \mu(1+\delta) ,$$
$$\mathbf{e}_3 = \frac{1}{\sqrt{2}} \left[\frac{M_Z \sin\theta_W (\cos\beta + \sin\beta)}{M_1 - \mu} , \frac{M_Z \cos\theta_W (\cos\beta + \sin\beta)}{\mu - M_2} , 1, -1+\epsilon \right] , \tag{6c}$$

$$m_4 = -\mu(1+\delta') \,, \tag{6d}$$

$$\mathbf{e}_4 = \frac{1}{\sqrt{2}} \left[\frac{M_Z \sin\theta_W (\cos\beta - \sin\beta)}{M_1 + \mu} \,, \right.$$

$$\left. \frac{M_Z \cos\theta_W (\sin\beta + \cos\beta)}{M_2 + \mu}, 1, 1+\epsilon' \right] .$$

Note that Eq. (5) implies $|m_2| > |m_1|$; $\mathbf{e}_2$ therefore never corresponds to the LSP. In the limit where either $|M_1|$ or $|\mu|$ (or both) is much bigger than M_Z, the LSP is therefore an almost pure b-ino ($\mathbf{e}_1$), or an almost pure antisymmetric or symmetric Higgsino ($\mathbf{e}_{3,4}$).[4]

The corrections δ, δ', ϵ, and ϵ' are formally $O(M_Z^2)$; however, they can be numerically quite important for a light Higgsino-like LSP. They are given by

$$\delta = \frac{M_Z^2(1+\sin 2\beta)}{2\mu} \left[\frac{\sin^2\theta_W}{\mu - M_1} + \frac{\cos^2\theta_W}{\mu - M_2} \right] ; \tag{7a}$$

$$\delta' = \frac{M_Z^2(1-\sin 2\beta)}{2\mu} \left[\frac{\sin^2\theta_W}{\mu + M_1} + \frac{\cos^2\theta_W}{\mu + M_2} \right] ; \tag{7b}$$

$$\epsilon = -\delta \frac{\cos 2\beta}{1+\sin 2\beta} \,; \tag{7c}$$

$$\epsilon' = -\delta' \frac{\cos 2\beta}{1-\sin 2\beta} \,. \tag{7d}$$

After inclusion of these terms one therefore finds that the mass splitting between the two Higgsino-like states is given by (in the limit $|M_1| \gg |\mu|$)

$$\| m_3 | - | m_4 \| = \frac{8 M_Z^2 \sin^2\theta_W}{3|M_1|} \left[1 + O\left(\frac{\mu}{M_1}, \frac{M_Z}{M_1} \right) \right] . \tag{8}$$

More details about neutralino masses and mixings can be found, e.g., in Refs. [17,42–44].

What are the final states into which a pair of neutralinos can annihilate? Here we only include two-body final states that can be produced in leading order of perturbation theory. From unsuccessful sparticle searches at LEP [45] as well as the bound $m_{\tilde{g}} > 120$ GeV that follows from the preliminary gluino search limit of the Collider Detector at Fermilab (CDF) Collaboration [46] after inclusion of "cascade decays" [47], one can derive [48] the bound $m_\chi \geq 20$ GeV.[5] We see that the annihilation $\chi\chi \to f\bar{f}$ is always kinematically allowed for all light SM fermions up to and including b quarks. For heavier neutralinos annihilation into a pair of gauge bosons also has to be included [18,19]. In addition the model contains at least one neutral scalar Higgs boson h with mass not much above M_Z, even after inclusion of radiative corrections [30]; the second neutral scalar H, the pseudoscalar P and the charged Higgs boson H^+ can also be accessible. In general one therefore also has to include annihilation into two Higgs bosons [18,19], as well as into one Higgs boson and one gauge boson.

We will now discuss annihilation into these final states in a little more detail, assuming χ to be either a nearly pure b-ino or a nearly pure Higgsino. Here we only give symbolic expressions for the matrix elements, which allow to estimate the order of magnitude of the various contributions; exact expressions for the cross sections for a general χ state are listed in Appendix A. Since we expand the annihilation cross section of Eq. (2) only up to $O(v^2)$, we only have to include s and p-wave contributions. s-wave contributions start at $O(v^0)$, but also contain $O(v^2)$ terms that contribute to Eq. (2) via interference with the $O(v^0)$ terms. p-wave matrix elements start at $O(v)$, so that we only need the leading term in the expansion. Of course, there is no interference between s- and p-wave contributions, and hence no $O(v)$ term in Eq. (2). Notice finally that Fermi statistics forces the s-wave state of two identical Majorana fermions to have $CP = -1$, while the p wave has $CP = +1$; the same argument also implies that the s wave has to have total angular momentum $J = 0$.

1. $\chi\chi \to f\bar{f}$

This reaction proceeds via the s-channel exchange of a Z or Higgs boson, as well as via sfermion exchange in the t channel. Each chirality state of f has its own superpartner with in general different mass, which mix [49] if the Yukawa coupling of f is not negligible. In the following expressions summation over both sfermions is always understood. Note that both the $Z-f-\bar{f}$ and fermion-sfermion-gaugino couplings conserve chirality; the sfermion and Z exchange contributions to the s-wave matrix element $\mathcal{M}_s$ are therefore proportional to the mass m_f of the final-state fermions. Contributions from Higgs-boson exchange, from the Higgsino-sfermion-fermion Yukawa interactions, and from sfermion mixing violate chirality, but have an explicit factor of m_f. The coefficient a in the expansion (2) of the annihilation cross section is therefore always proportional to m_f^2 for this final state, independent of the composition of χ. Moreover, since the CP quantum number of the exchanged Higgs boson must match that of the initial state, only P exchange contributes to $\mathcal{M}_s$, while h and H exchange contribute to $\mathcal{M}_p$. Since $\mathcal{M}_p$ only contributes to the coefficient b in Eq. (2), which is suppressed by a factor $3/x_F \simeq 0.1-0.2$, P exchange is potentially much more important than the contribution from the scalar Higgs bosons.

For a b-ino-like LSP the matrix elements thus have the structure

[4]Unless $|M_1| \simeq |\mu|$, in which case strong Higgsino–b-ino mixing occurs. Such mixed states always lead to very small relic densities [18,22,33,26].

[5]We note in passing that this implies a freeze-out temperature $T_F \geq 1$ GeV, well above the temperature where the quark-hadron phase transition is expected to occur. Our results do therefore not depend on the exact value of the critical temperature for this phase transition, in contrast with the case of a very light LSP [36].

$$\mathcal{M}_s(\chi\chi\to f\bar{f})|_{b\text{-ino}} \propto g'^2 m_f \left[c_1 \frac{m_\chi}{m_{\tilde{f}}^2+m_\chi^2} Y_f^2 + c_2 \frac{M_Z^2}{M_1^2-\mu^2}\frac{m_\chi}{M_Z^2} + c_3 \frac{1}{M_1+\mu}\frac{m_\chi^2}{4m_\chi^2-m_P^2+im_P\Gamma_P} \right] ; \tag{9a}$$

$$\mathcal{M}_P(\chi\chi\to f\bar{f})|_{b\text{-ino}} \propto g'^2 v \left[d_1 \frac{m_\chi^2}{m_{\tilde{f}}^2+m_\chi^2} Y_f^2 + d_2 \frac{M_Z^2}{M_1^2-\mu^2}\frac{m_\chi^2}{4m_\chi^2-M_Z^2+iM_Z\Gamma_Z} + \sum_{i=1}^{2} d_{3,i}\frac{m_f}{M_1+\mu}\frac{m_\chi^2}{4m_\chi^2-M_{H_i}^2+iM_{H_i}\Gamma_{H_i}} \right] . \tag{9b}$$

Here the c_i and d_i are numerical constants of order 1, and g' is the $U(1)_Y$ gauge coupling. c_3 and the $d_{3,i}$ describe the Higgs-boson–$f\bar{f}$ couplings, where we have introduced the notation [42] $H_1=H$, $H_2=h$; in certain cases some of these couplings can be enhanced [42] by a factor $\tan\beta$ (or suppressed by $\cot\beta$).

We see from Eqs. (9) that the s-channel diagrams are all suppressed by small couplings. The Z boson couples to neutralinos only via their Higgsino components; more precisely,

$$g_{Z\chi_i\chi_j} \propto e_{i,3}e_{j,3} - e_{i,4}e_{j,4} , \tag{10}$$

where $e_{i,l}$ is the lth component of $\mathbf{e}_i$ [see Eqs. (6)]. For a b-ino-like state this coupling is doubly suppressed, as indicated in Eqs. (9). The Higgs boson couplings to neutralinos originate from the Higgs-boson–Higgsino–gaugino gauge interaction terms of the unmixed Lagrangian; for a b-ino-like neutralino this coupling involves therefore only one factor of the (small) Higgsino component. Finally, the sfermion exchange contributions can only be suppressed by choosing $m_{\tilde{f}}^2 \gg m_\chi^2$ in this case.

For a Higgsino-like LSP, Eqs. (9) become

$$\mathcal{M}_s(\chi\chi\to f\bar{f})|_{\text{Higgsino}} \propto (g^2+g'^2) m_f \left[\left[c_1' \frac{M_Z}{\mu+M} + c_1'' \frac{m_f}{M_Z} \right]^2 \frac{m_\chi}{m_{\tilde{f}}^2+m_\chi^2} + c_2' \frac{M_Z^2}{\mu M}\frac{m_\chi}{M_Z^2} + c_3' \frac{1}{M_1+\mu}\frac{m_\chi^2}{4m_\chi^2-m_P^2+im_P\Gamma_P} \right] ; \tag{11a}$$

$$\mathcal{M}_p(\chi\chi\to f\bar{f})|_{\text{Higgsino}} \propto (g^2+g'^2) v \left[\left[d_1' \frac{M_Z}{\mu+M} + d_1'' \frac{m_f}{M_Z} \right]^2 \frac{m_\chi^2}{m_{\tilde{f}}^2+m_\chi^2} + c_2' \frac{M_Z^2}{\mu M}\frac{m_\chi^2}{4m_\chi^2-M_Z^2+iM_Z\Gamma_Z} + \sum_{i=1}^{2} d_{3,i}''\frac{m_f}{M_1+\mu}\frac{m_\chi^2}{4m_\chi^2-m_P^2+im_P\Gamma_P} \right] . \tag{11b}$$

Notice that Eqs. (11) also get contributions from SU(2) gauge interactions, which enter Eqs. (9) only in higher orders in $M_Z/(M+\mu)$. On the other hand, the sfermion exchange contribution is now suppressed by either the small gaugino component of the LSP, see Eqs. (6c) and (6d), or by a power of the Yukawa coupling; of course, for $f=t$ the latter is hardly a suppression, and can even be an enhancement if the top quark is heavy. In contrast, Higgs-boson exchange contributes at the same order [in $M_Z/(M_1+\mu)$] to the annihilation of b-ino-like and Higgsino-like LSP's.[6] Finally, the Z exchange contribution again behaves quite differently in the two cases of Eqs. (9) and (11): While in the former case, it decreases quadratically with the mass of the heavy neutralinos (whose mass is $\propto\mu$, in this case), Eqs. (7) and (10) show that the $Z\chi\chi$ coupling for a Higgsino-like LSP decreases only linearly with the mass of the heavy neutralinos (with mass $\propto M$).[7] Moreover, Eqs. (6) and (10) imply that the off-diagonal $Z\chi\chi'$ coupling is not suppressed at all if $\chi=\mathbf{e}_3$, $\chi'=\mathbf{e}_4$, or vice versa. If Z exchange gives the dominant contribution (which is true for light Higgsinos, except in the vicinity of the h pole), one therefore has

$$\sigma(\chi\chi'\to f\bar{f}) \propto \left[\frac{M_1\mu}{M_Z^2} \right]^2 \sigma(\chi\chi\to f\bar{f}) . \tag{12}$$

In this case $\chi\chi'$ coannihilation [37] can be quite impor-

[6]The fact that the Higgs coupling to a mixed neutralino is unsuppressed explains to a large part the big annihilation cross sections, and hence small relic densities, of this kind of LSP.

[7]Unitarity implies that the $Z\chi\chi$ coupling must be suppressed at least like $1/m_\chi$ as $m_\chi\to\infty$. The Z exchange contribution to $\mathcal{M}_s$ behaves like $g_{Z\chi\chi}m_f m_\chi/M_Z^2$. This contribution cannot be canceled by $\tilde{f}$ or P exchange because one can always choose $m_{\tilde{f}}, m_P \gg m_\chi$; since this does not increase any couplings, the heavy states simply decouple in this limit. The Z coupling itself therefore has to compensate for the factor of m_χ.

tant [26]; we will come back to this point later.

2. $\chi\chi \to W^+W^-, ZZ$

These final states can be produced via t-channel chargino or neutralino exchange, as well as s-channel exchange of scalar Higgs bosons; in case of the W^+W^- final-state s-channel Z exchange also contributes. It is important to realize here that the cross sections behave quite differently for longitudinal and transverse gauge bosons. For each longitudinal gauge boson the amplitude gets an enhancement factor $\gamma_V = E_V/M_V \simeq m_\chi/M_V$. Unitarity then requires strong cancellations between different contributions to the matrix element if the couplings of χ to V are not suppressed. On the other hand, these enhancement factors can give finite matrix elements in the limit $m_\chi \to \infty$ even if the couplings do vanish in this limit. These effects can also be understood from the equivalence theorem [50], which states that in the high-energy limit, the matrix element for the production of a longitudinal gauge boson is identical to the one for the production of the would-be Goldstone boson that gets "eaten" when the gauge boson acquires its mass. The couplings of these Goldstone modes to neutralinos and charginos originate from the Higgs-boson–Higgsino–gaugino gauge interactions of the unmixed Lagrangian. This means that a pair of would-be Goldstone bosons can be produced with full gauge strength from pure gaugino as well as pure Higgsino initial states, by exchange of Higgsinos or gauginos, respectively. On the other hand, since the relevant couplings are gauge couplings, the matrix element must be well behaved in the limit where any mass becomes very large. Notice finally that neither a pair of longitudinal gauge bosons nor a combination of one longitudinal and one transverse gauge boson can exist in a $J=0$ state with $CP=-1$; these final states are therefore only accessible to the p-wave initial state.

For a b-ino-like LSP, the coupling to gauge bosons does indeed decrease like $1/m_\chi$ [see Eq. (6a)]. The above discussion then shows that only the amplitude for the production of two longitudinal gauge bosons survives, which is purely p wave ($V=W,Z$):

$$\mathcal{M}_p(\chi\chi \to VV)|_{b\text{-ino}} \propto g'^2 v \left[d_4 \frac{M_Z^2}{M_1^2+\mu^2} \frac{m_\chi}{\mu} + \sum_{i=1}^{2} d_{5,i} \frac{M_Z}{M_1+\mu} \frac{m_\chi M_V}{4m_\chi^2 - m_{H_i}^2 + i m_{H_i}\Gamma_{H_i}} \right] \frac{m_\chi^2}{M_V^2} . \tag{13}$$

Because of the enhancement factor γ_V^2, the annihilation of heavy b-ino-like LSP's into (longitudinal) gauge bosons does *not* vanish for $m_\chi \to \infty$, unless one has $|M_1| \ll |\mu|$. Considering [19] an exact b-ino state therefore does not give the right answer in this case. As discussed above, this can also be understood from the equivalence theorem, since the production of two Goldstone modes can only be suppressed by making the exchanged Higgsino very heavy. (This argument is made more rigorous in Appendix B, where numerical factors from the diagonalization of the Higgs sector, etc., are treated properly.) Finally, we mention that the coefficient $d_{5,1}$ is often quite small, since the heavy Higgs scalar decouples [42] from W and Z bosons when its mass is large. In contrast, the exchange of the light Higgs boson actually gives the dominant contribution in the limit $|\mu| \gg |M_1|$.

For a Higgsino-like LSP one has

$$\mathcal{M}_s(\chi\chi \to VV)|_{\text{Higgsino}} \propto (g^2+g'^2) c_4' ; \tag{14a}$$

$$\mathcal{M}_p(\chi\chi \to VV)|_{\text{Higgsino}} \propto (g^2+g'^2) v \left[d_4' + \sum_{i=1}^{2} d_{5,i}' \frac{M_Z}{M+\mu} \frac{m_\chi M_V}{4m_\chi^2 - m_{H_i}^2 + i m_{H_i}\Gamma_{H_i}} \frac{m_\chi^2}{M_V^2} \right] . \tag{14b}$$

Notice that in this case there is no propagator suppression of the t-channel diagrams for $V_T V_T$ production, because the exchanged (other) Higgsino state is almost mass degenerate with the LSP. Since the (off-diagonal) couplings to gauge bosons are not suppressed in this case, cancellations between t-channel (and Z exchange, for $V=W$) diagrams are necessary to restore unitarity for $V_L V_L$ production. The equivalence theorem shows that in the limit $|M_1| \gg |\mu|$ the contribution from longitudinal gauge bosons is even suppressed, since the production of Goldstone bosons necessitates the exchange of heavy gauginolike states, or the exchange of Z or Higgs bosons whose diagonal couplings are also suppressed in this limit. Moreover, the production of $V_L V_T$ final states is suppressed by neutralino mixing factors. However, the production of transverse gauge bosons, and hence the total cross section, is not suppressed in the limit where the masses of the heavier neutralinos become very large; this is again in contrast to the case of a b-ino-like LSP.[8]

[8]The $V_L V_L$ final states have not been treated properly in Ref. [19]. However, since they only contribute to p-wave annihilation, they are numerically not very important. This is even true for b-ino-like LSP's where the production of transverse gauge bosons does not contribute, since here the total annihilation cross section is dominated by the $f\bar{f}$ final state.

3. $\chi\chi \to Zh$

This final state can be produced via neutralino exchange in the t-channel as well as s-channel exchange of Z and P bosons. Notice that now a longitudinal Z boson can be produced both from the s and p wave; since we always need at least one neutralino mixing factor, the matrix element would go to zero in the limit of large LSP mass without the enhancement factor γ_Z. For the case of a b-ino-like LSP, the matrix elements have the form

$$\mathcal{M}_s(\chi\chi \to Zh)|_{b\text{-ino}} \propto g'^2 \frac{m_\chi}{M_1+\mu} \frac{M_Z^2}{m_P^2+M_Z^2} \times \left[c_6 + c_7 \frac{m_\chi^2}{4m_\chi^2 - m_P^2 + i m_P \Gamma_P} \right] ; \tag{15a}$$

$$\mathcal{M}_p(\chi\chi \to Zh)|_{b\text{-ino}} \propto g'^2 v d_6 \frac{m_\chi^2}{M_1^2+\mu^2} . \tag{15b}$$

Both c_6 and d_6 get contributions from neutralino as well as Z exchange diagrams; in the important limit $m_P^2 \gg M_Z^2$, $\mathcal{M}_s$ is strongly suppressed, due to a cancellation between the two classes of diagrams. In this limit the ZhP coupling also becomes small [42], suppressing the P exchange contribution as indicated. Only the p-wave amplitude (15b) therefore survives in the limit $m_P^2 \gg M_Z^2$. Notice, however, that the amplitude as a whole does not vanish in the limit of large sparticle masses and small neutralino mixing, unless $|\mu| \gg |M_1|$; once again this is due to the production of a longitudinal gauge boson, giving rise to an enhancement factor m_χ/M_Z.

For a Higgsino-like LSP Eqs. (15) become

$$\mathcal{M}_s(\chi\chi \to Zh)|_{\text{Higgsino}} \propto (g^2+g'^2) \frac{m_\chi}{M+\mu} \left[c_6' + c_7' \frac{M_Z^2}{m_P^2+M_Z^2} \frac{m_\chi^2}{4m_\chi^2 - m_P^2 + i\Gamma_P m_P} \right] , \tag{16a}$$

$$\mathcal{M}_p(\chi\chi \to Zh)|_{\text{Higgsino}} \propto (g^2+g'^2) v d_7' \frac{m_\chi^2}{M^2+\mu^2} . \tag{16b}$$

Note that in this case the $O(v^0)$ term from the t-channel and Z exchange diagrams is *not* suppressed for $m_P^2 \gg M_Z^2$. Just as in the case of a b-ino-like LSP the total amplitude is only suppressed if the heavier neutralinos are much heavier than m_χ, i.e., if $|M_1| \gg |\mu|$ in this case.

4. $\chi\chi \to hh$

Here only t-channel neutralino exchange and s-channel scalar Higgs-boson exchange diagrams contribute. Since two identical scalars cannot be in a state with $J=0$ and $CP=-1$, annihilation can only proceed from the p wave. The amplitude thus has the general form

$$\mathcal{M}_p(\chi\chi \to hh) \propto g'^2 v \left[d_8 \frac{m_\chi}{M+\mu} + d_9 \frac{M_Z^2}{M^2-\mu^2} + \sum_{i=1}^{2} d_{10,i} \frac{M_Z}{M+\mu} \frac{M_Z m_\chi}{4m_\chi^2 - m_{H_i}^2 + i m_{H_i} \Gamma_{H_i}} \right] . \tag{17}$$

This form holds for both b-ino-like and Higgsino-like LSP's. The contribution $\propto d_8$ comes from the exchange of the heavier neutralinos, which occurs with full gauge strength but is suppressed by small propagators; the term $\propto d_9$ originates from neutralino mixing. In case of a b-ino-like LSP the coefficient d_8 is suppressed if $\tan\beta \gg 1$ and $|\mu| \gg |M_1|$:

$$d_{8,b\text{-ino}} = d_8' \frac{M_1 + \mu \sin 2\beta}{\mu} . \tag{18}$$

This possible additional suppression is absent for the case of a Higgsino-like LSP; in this case the amplitude also gets contributions from SU(2) gauge interactions, as do all other higgsino annihilation amplitudes.

This concludes our qualitative discussion of the annihilation matrix elements for the most important final states. In principle, the heavier Higgs bosons H, P, and H^+ could also be produced [18,19] in $\chi\chi$ annihilation, either in pairs or in association with a gauge boson. However, we will see in the next subsection that in minimal supergravity models these heavy states are usually not accessible. We do therefore not discuss the relevant matrix elements here; of course, they are included in the list of matrix elements in Appendix A.

C. The particle spectrum

The basic assumption of minimal supergravity (SUGRA) models is that supersymmetry breaking can be described [7] in terms of just three parameters: A universal scalar mass m, a universal gaugino mass M, and a universal parameter A characterizing the strength of nonsupersymmetric trilinear scalar interactions. If the particle spectrum is restricted to that of the MSSM, which we always assume in this paper, one in addition has to introduce a supersymmetric contribution μ to Higgs boson and Higgsino masses; the masses μ_1 and μ_2 of the two Higgs doublets are then given by

$$\mu_1^2=\mu_2^2=m^2+\mu^2 , \tag{19}$$

while the Higgs mixing term μ_3^2 is given by

$$\mu_3^2=(A-m)m . \tag{20}$$

This simple form of the particle spectrum is assumed to emerge after integrating out the fields of the "hidden sector" [7] where local supersymmetry is broken spontaneously. Since the decoupling of these fields occurs at the Planck or grand unified theory (GUT) scale the spectrum will be this simple only at ultrahigh energies $Q \geq M_X$; in particular, Eq. (19) will only hold at these very high energies.

Of course, present day experiments, as well as DM annihilation, occur at much smaller energy scales. The particle spectrum at energies of the order of the weak or sparticle mass scale can be obtained by solving a set of coupled renormalization-group equations (RGE's) [10]; for given m, M, A, μ, and Yukawa couplings h_t, h_b (with $h_b=h_\tau$ at the GUT scale), minimal SUGRA specifies the boundary conditions at $Q=M_X$, which uniquely determine the particle spectrum at lower energies. In this scheme leading logarithms are automatically summed; i.e., all terms of order $[(\alpha/\pi)\ln M_X/M_Z]^n$ are automatically included, where α is a generic gauge or Yukawa coupling. It has been recognized quite early [10,51] that the radiative corrections described by the RGE can induce spontaneous breaking of the $SU(2)\times U(1)_Y$ gauge symmetry by driving some combination of the squared Higgs-boson mass parameters μ_i^2 of Eq. (19) to negative values. This is due to the effect of the Yukawa couplings, which tend to reduce the squared masses of scalar fields. The Yukawa sector therefore plays a crucial role in these models.

In a recent paper [32] we studied radiative gauge symmetry breaking and the particle spectrum in minimal SUGRA in some detail, taking care to incorporate the effects of the Yukawa couplings of the b quark and τ lepton, which can be quite important if $|\tan\beta| \gg 1$. We later showed [52] how to incorporate the "finite" (i.e., without $\ln M_X/M_Z$ enhancement) radiative corrections to the Higgs sector in this scheme. In particular, we demonstrated that for most purposes these radiative corrections can be made negligibly small by a proper choice of the scale Q_0 where the RG running is terminated; the only exception is the mass m_h of the light Higgs scalar where the corrections have to be included explicitly. (A similar result had been obtained previously in Ref. [53].) For more details we refer the reader to these papers, as well as to earlier work on this subject [10,51]; here we only give a brief summary of the relevant properties of the spectrum.

As stated above, the squared mass of all sfermions at the GUT scale is simply given by m^2. In case of the superpartners of the first two generations the only sizable radiative corrections to the masses involve the gauge interactions. The breakdown on $SU(2)\times U(1)_Y$ gauge symmetry also has some effect on sfermion masses. All these contributions can quite easily be computed analytically; one has

$$m_{\tilde{f}_i}^2=m^2+d_i M^2+\cos 2\beta(I_{3,i}-Q_i\sin^2\theta_W)M_Z^2 , \tag{21}$$

where $I_{3,i}$ and Q_i are the third component of the weak isospin and electric charge of the sfermion $\tilde{f}_i$, respectively. The positive constant d_i is determined by the gauge quantum numbers of the sfermion; numerically, it is about six for squarks, 0.5 for SU(2)-doublet sleptons, and 0.15 for SU(2)-singlet sleptons with hypercharge 1.

The gaugino masses M_i are all equal to M at scale M_X; their Q dependence is identical to that of the gauge couplings α_i:

$$M_i(Q)=\frac{\alpha_i(Q)}{\alpha_i(M_X)}M , \tag{22}$$

which immediately implies Eq. (5). Numerically, $M_3 \simeq 3M$, $M_2 \simeq 0.84M$, and $M_1 \simeq 0.43M$.[9]

Equations (21) and (22) have been taken into account in some previous analyses [20–22,24,25] of LSP relic densities. Unfortunately, the effects of the Yukawa couplings are not so easily treated analytically. These effects are important for the masses of third-generation sfermions as well as Higgs bosons. Indeed, Yukawa couplings affect sfermion masses already at the tree level [49]; they lead to mixing between SU(2)-doublet and -singlet sfermions, and give rise to additional supersymmetric diagonal mass terms. These effects are especially important for top squarks, which obviously have the largest Yukawa couplings; this has been included in the analysis of Ref. [23]. However, for $|\tan\beta| \gg 1$, bottom-squark and especially τ-slepton mixing also becomes important [32]. Moreover, the Yukawa couplings reduce the nonsupersymmetric diagonal mass terms from the values predicted by Eq. (21). The net effect is that the lighter top-squark and τ-slepton eigenstates can be substantially lighter than the other squarks and sleptons, respectively; indeed, no strict lower bound on these masses could be given even if the masses of first generation sfermions were known. The maximal reduction of the light bottom-squark mass is not quite as large, but can still amount to 20–30% if $|\tan\beta| \simeq m_t/m_b$. Since tree-level and loop effects tend to cancel for the heavier eigenstates of third-generation sfermions, their masses are usually not very different from those of the corresponding sfermions of the first two generations.

The Yukawa couplings also affect the Higgs-boson masses via the RGE; as explained above, this effect is at the heart of the radiative gauge symmetry-breaking mechanism. First of all, it should be noted that the masses of the heavier Higgs bosons are related to the sfermion masses via Eq. (19); this equation only holds at scale

[9]In our numerical calculations we use proper on-shell masses, i.e., $m_{\tilde{f}_i} \equiv m_{\tilde{f}_i}(Q=m_{\tilde{f}_i})$ and similar for gluinos. The coefficients in Eqs. (21) and (22) then depend on the masses themselves, rather than being simple constants. This can change the masses of strongly interacting sparticles by as much as 20%; e.g., for 1-TeV gluinos, $m_{\tilde{g}} \simeq 2.5|M|$, rather than $3|M|$.

M_X, but it shows that in SUGRA models one cannot treat Higgs boson and sfermion masses as independent free parameters. As well known [54], the masses of the P, H, and H^+ states are essentially determined by m_P, which is simply given by

$$m_P^2=\mu_1^2(Q_0)+\mu_2^2(Q_0)\ ; \tag{23}$$

as discussed above, Eq. (23) also holds to good approximation after inclusion of one-loop radiative corrections if the scale Q_0 where the RG running is terminated is chosen properly, i.e., $Q_0\simeq m_{\tilde{q}}$. Notice that only the Higgs doublet H_2 couples to top quarks; moreover, the requirement

$$\langle H_1^0\rangle^2+\langle H_2^0\rangle^2=2M_W^2/g^2 \tag{24}$$

immediately implies [10] $\mu_2^2(Q_0)>-M_Z^2/2$. If the b and τ Yukawa couplings are neglected, the nonsupersymmetric contribution to μ_1^2 runs just like an SU(2)-doublet slepton mass; i.e., it *increases* when going from $Q=M_X$ to $Q=Q_0$; in addition the positive supersymmetric contribution μ^2 has to be added.[10] This argument shows that m_P can only be smaller than the slepton masses if the b and τ Yukawa couplings are sizable, i.e., if $|\tan\beta|\gg 1$. The exact numerical expression for m_P can be approximated by [32]

$$m_P^2=\frac{M_Z^2}{2}(\cot\beta-1)+[m^2+0.52M^2+\mu^2(Q_0)]\times\left[\frac{1}{\sin^2\beta}-\frac{a^2}{\cos^2\beta}\right], \tag{25}$$

where $a\simeq\frac{1}{45}-\frac{1}{35}$ depends on the ratios M/m and A/m as well as on the top mass m_t.[11]

The mass of the lightest Higgs scalar h in general depends on all parameters of the model in a complicated way. However, in the important limit $m_P^2\gg M_Z^2$ the situation simplifies greatly, and one finds [52]

$$m_h^2=M_Z^2\cos^2 2\beta+\Delta_{22}\sin^2\beta+O\left[\frac{M_Z^2}{m_P^2},\frac{m_b^2}{m_t^2}\right]. \tag{26}$$

Here Δ_{22} describes the leading radiative corrections from top-quark–top-squark loops. It grows like the fourth power of m_t, but depends only rather mildly on the values of the SUSY-breaking parameters; in the limit $m_{\tilde{q}}^2\gg m_t^2$ it grows $\propto\ln m_{\tilde{q}}/m_t$.

The SUGRA-imposed constraint that is most difficult to treat analytically follows from the almost obvious observation that in the radiative gauge symmetry-breaking scenario the VEV's of the Higgs fields can be computed from the input parameters at the GUT scale; i.e., $\langle H_{1,2}^0\rangle$ are functions of m, M, A, μ, and the set of Yukawa couplings h_t, h_b, h_τ. The condition (24) therefore leads to a relation between these parameters. This relation cannot be expressed in closed form once the effects from $h_{b,\tau}$ are included, but it can approximately be written as [32]

$$\mu^2(Q_0)\simeq\frac{\tan^2\beta+1}{\tan^2\beta-1}X_2-m^2-0.52M^2-M_Z^2/2\ , \tag{27}$$

where X_2 describes the effect of the RG running due to the top-quark Yukawa coupling. An approximate expression for X_2 is[12]

$$X_2\simeq\left[\frac{m_t}{150\text{ GeV}}\right]^2\left\{0.9m^2+2.7M^2+\left[1-\left[\frac{m_t}{190\text{ GeV}}\right]^3\right]\times(0.24A^2+MA)\right\}. \tag{28}$$

Equation (27) usually works to 10% accuracy, but Eq. (28) might deviate by as much as 20% from the exact numerical result; nevertheless, these expressions are quite useful to gain some insight into the relation between the input parameters.

Strictly speaking, Eq. (27) does not provide the searched-for relation between input parameters at scale M_X on the one hand and M_Z on the other, since it still depends on $\tan\beta$, which is itself a complicated function of the input parameters. (In fact, this is where the dominant effect from the other Yukawa couplings enters.) However, μ^2 becomes essentially independent of $\tan\beta$ if $\tan^2\beta\gg 1$, in practice for $|\tan\beta|>3$ or so. Another complication arises because a given set of m, M, A, and m_t often allows up to three different solutions [32] of the equation that determines $\tan\beta$ (and hence the Yukawa couplings); these solutions differ in both sign and magnitude of $\tan\beta$.[13] We therefore present results always for fixed $\tan\beta$, M, and m, rather than fixing the values of the SUSY-breaking parameters. Since consistent solutions only exist for $h_t>h_b$, the allowed range of $\tan\beta$ in this model is restricted to $1<|\tan\beta|<m_t/m_b$.

---

[10]Note that this is the square of the real parameter μ, which renormalizes multiplicatively; μ^2 is therefore indeed always positive.

[11]In Ref. [32] we gave a somewhat larger numerical value of a, because we underestimated the effect of the running of the b-quark mass between Q_0 and m_b. Since a smaller $m_b(Q_0)$ also implies a larger upper bound on $|\tan\beta|$, our results for sparticle masses, including $m_{\tilde{b}}$, remain valid if one rescales $\tan\beta\to 1.15\tan\beta$ in the region $|\tan\beta|\gg 1$.

[12]In Ref. [32] we gave a somewhat larger expression for X_2, since we had chosen a rather small value for Q_0, i.e., $Q_0=M_Z$; Eq. (28) is valid for $Q_0\simeq 300$ GeV.

[13]In this scheme the sign of $\tan\beta$ is determined dynamically via the RGE. On the other hand, the couplings listed in Refs. [6] and [42] have been derived under the assumption $\tan\beta>0$. Fortunately, the masses and mixings of the neutralino and chargino eigenstates only depend on the sign of the product $M\mu\tan\beta$; a sign in $\tan\beta$ can therefore always be "rotated" into M or μ.

Unfortunately another twofold ambiguity occurs when μ and A are adjusted such that M_Z and $\tan\beta$ have their desired values. In one of these solutions μ is of the order of m and M. However, unless m_t is very large there is also a second solution with $\mu^2 \ll m^2, M^2$; indeed, this is the "small μ" solution which has been discussed in the first analyses [10] of radiative gauge symmetry breaking. However, by now this kind of solution is quite severely constrained. First of all, we know from SUSY searches at LEP [45] that $|\mu(Q_0)| > 40$ GeV; since these solutions typically have $|\mu|$ much smaller than m and M, this constraint implies that most sparticles must be quite heavy for these solutions to be acceptable. Moreover, for $m_t > 155$ GeV the small-μ solutions disappear altogether, since then the effect of the top-quark Yukawa coupling always drives $\mu_2^2(Q_0)$ below $-M_Z^2/2$ unless it receives a sizable, positive contribution $+\mu^2$ [see Eq. (19)].

At this point some comments on fine-tuning might be appropriate. It should be quite obvious that the "natural" scale for the VEV's of the Higgs fields is set by the dimensionful parameters of the Higgs potential, which in turn are roughly of the order of typical sparticle masses, as can be seen from Eqs. (23) and (27). Therefore some fine-tuning of parameters will be necessary [35,16] to achieve $M_Z^2 \ll m^2 + M^2$. This provides a strong argument that sparticles should not be much heavier than ~ 1 TeV, but this argument cannot be translated into strict upper bounds on sparticle masses. Since one of the motivations of this study is to see whether cosmology might provide us with such bounds, we do not impose any "*a priori*" upper bounds on the SUSY-breaking parameters in our analysis. One might also argue that large ratios of the mass parameters of the model are "unnatural," but the Yukawa sector shows that large ratios of "fundamental" parameters can indeed occur. Of course, one ultimately hopes to understand the origin of the dimensionful parameters m, M, A, and μ better, e.g., in the framework of superstring theories [55]. However, at present it seems safer to pursue an "agnostic" approach, and try to cover the *entire* experimentally allowed parameter space.

This allowed region is defined via the experimental constraints

$$m_{\tilde{e}_{R,L},\tilde{\tau}_1,\tilde{t}_1,\tilde{\chi}^+} > 45 \text{ GeV} , \tag{29a}$$

$$m_{\tilde{\nu}} > 40 \text{ GeV} , \tag{29b}$$

$$\sum_{i,j=1}^{4} B(Z \to \tilde{\chi}_i^0 \tilde{\chi}_j^0) < 5 \times 10^{-5} , \tag{29c}$$

$$\Gamma(Z \to \tilde{\chi}_1^0 \tilde{\chi}_1^0) < 12 \text{ MeV} , \tag{29d}$$

$$m_{\tilde{g}} > 120 \text{ GeV} , \tag{29e}$$

$$m_{\tilde{\tau}_1} \geq m_\chi . \tag{29f}$$

The bounds (29a)–(29d) directly follow from LEP limits on sparticle production [45] as well as on the invisible width of the Z boson; here $\tilde{\chi}^+$ and $\tilde{\chi}_i^0$ stand for a generic chargino and neutralino state, with $\tilde{\chi}_1^0 \equiv \chi$. The bound (29e) is a conservative interpretation of the preliminary CDF search limits [46] after inclusion of cascade decays [47]. Finally, (29f) follows directly from the requirement that the LSP should not be charged, as discussed in the introduction. Further experimental constraints follow from the unsuccessful search of Higgs bosons; we have incorporated a parametrization of the ALEPH bound [56] in our list of conditions.

In addition to imposing these experimental constraints, we also discard combinations of parameters that lead to deeper lying minima of the scalar potential that break charge and/or color; this requirement excludes combinations with $A^2/(m^2+M^2) \gg 1$ [57]. Finally, we demand that the scalar potential should be bounded from below at scale $Q = M_X$, which implies $\mu_1^2 + \mu_2^2 \geq 2|\mu_3^2|$; Eq. (20) shows that this excludes the region

$$\frac{|B|}{2} - \left[\frac{B^2}{4} - m^2\right]^{1/2} < |\mu(M_X)| < \frac{|B|}{2} + \left[\frac{B^2}{4} - m^2\right]^{1/2} , \tag{30}$$

if $|B| \equiv |A - m| \geq 2m$. This constraint is effective at small $|\tan\beta|$, which implies large μ [see Eq. (27)] and thus large and positive squared Higgs-boson mass parameters (21). One then needs large $|A/m|$ to achieve spontaneous gauge symmetry breaking, since this accelerates the RG running of the mass parameters; however, large $|B/m|$ also imply a large excluded region (30).

III. EXAMPLES

We are now in a position to present some numerical results. The discussion of Sec. II C showed that the model has four free parameters, which we chose to be m, M, m_t, and $\tan\beta$; μ and A are then fixed by the equations describing the minimization of the Higgs potential, up to a possible discrete ambiguity. Without loss of generality m_t and m can be chosen to be positive, but M and $\tan\beta$ can have either sign.

Figures 1(a)–1(d) show a first partial exploration of the parameter space of the model. In these figures we have fixed $m = 300$ GeV, which leads to cosmologically interesting DM densities for a wide range of the remaining parameters. In addition, in each figure we have kept m_t and $\tan\beta$ fixed, and varied M. We find that for the chosen values of parameters only one experimentally allowed solution for A and μ exists. Moreover, since in all these cases the mass of the LSP increases monotonically with $|M|$, we present our results as a function of m_χ; this simplifies the identification of the various s-channel poles and of the thresholds where new annihilation channels open up. The starting point of all curves in Figs. 1 is determined by the LEP constraints (29a), (29c), and (29d).

We see that in the limit of large m_χ all curves become almost identical. The reason is that in this case we always have $|\mu| > |M_1| \gg M_Z$, so that the LSP is b-ino-like. The dominant annihilation channel is then $\chi\chi \to l^+ l^-$ via $\tilde{l}$ exchange, where l is any lepton. Equation (9) shows that squark exchange is suppressed [22] by their large mass (21), and the Z and Higgs-boson exchange contributions are suppressed by small couplings. As discussed in Sec. II B, the production of longitudinal gauge bosons V_L

and of the light Higgs boson h are not suppressed by powers of M_Z/m_χ, but are suppressed by powers of $|M_1/\mu| \simeq \frac{1}{4}-\frac{1}{2}$ for the examples of Figs. 1; moreover, all neutralino couplings relevant for these final states originate (either directly or via the equivalence theorem) from the Higgs-boson–Higgsino–gaugino $U(1)_Y$ gauge interaction, which involve fields with hypercharge $|Y|=\frac{1}{2}$, while the SU(2) singlet leptons have $Y=1$. The gauge and Higgs-boson final states therefore only contribute a few percent in the region $m_\chi > 200$ GeV [> 300 GeV for the dashed curve in Fig. 1(c); see below].

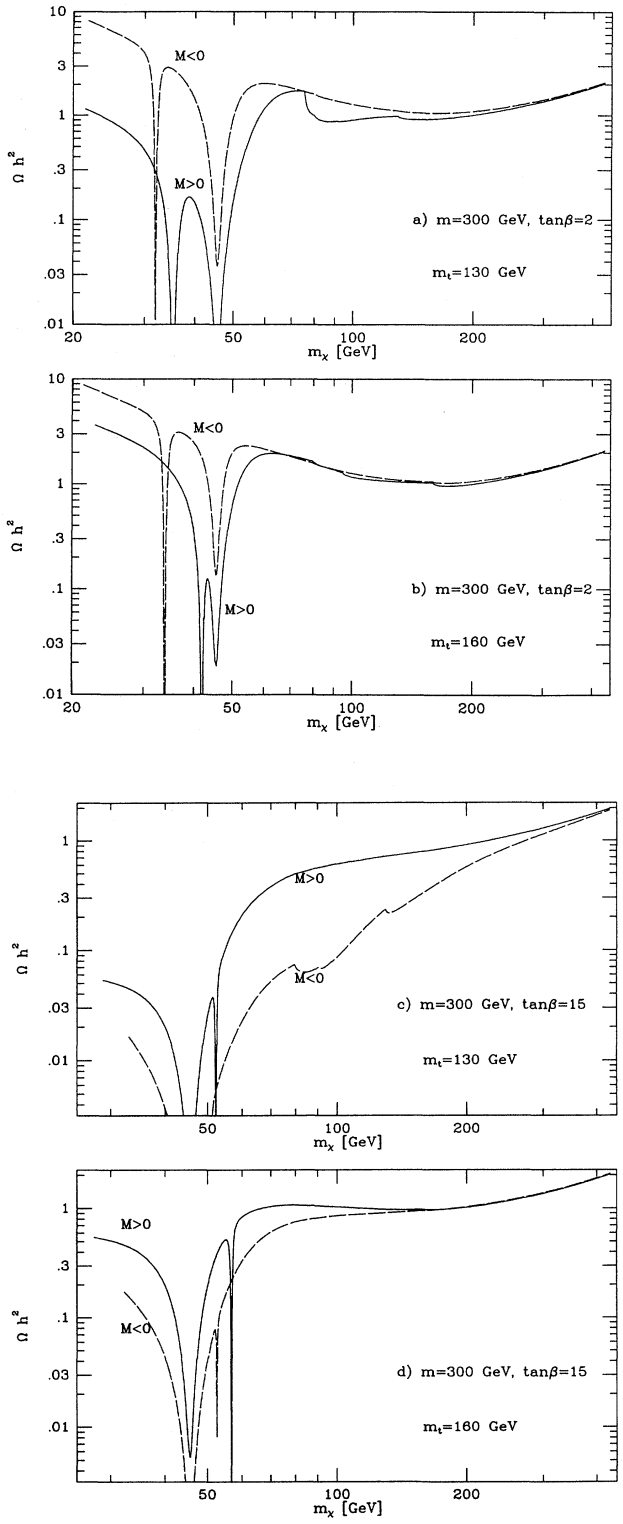

The behavior of the curves in this region can therefore be understood semiquantitatively from the $\tilde{l}_R$ exchange contribution alone:

$$\sigma_{\text{ann}} \propto \frac{m_\chi^2}{(m_{\tilde{l}_R}^2+m_\chi^2)^2}\left[\left[1-\frac{m_\chi^2}{m_{\tilde{l}_R}^2+m_\chi^2}\right]^2 + \frac{m_\chi^4}{(m_{\tilde{l}_R}^2+m_\chi^2)^2}\right], \tag{31}$$

where the parentheses result from the Taylor expansion of the propagator in powers of the velocity v. SUGRA predicts $m_{\tilde{l}_R}^2 \simeq m^2+0.83m_\chi^2$ for the given case of a b-ino-like LSP [see Eqs. (21) and (22)]; Eq. (31) then leads to a maximum of the annihilation cross section, i.e., a minimum of the relic density, at $m_\chi \simeq 0.6m \simeq 180$ GeV for the parameters of Figs. 1. This maximum is very broad; the $\tilde{l}_R$ exchange contribution falls to 50% of its maximal value at $m_\chi \simeq 1.52m$, just beyond the end of the region shown in Figs. 1. Indeed, in Figs. 1(a) and 1(b), Ωh^2 at $m_\chi = 430$ GeV is about twice as large as at the minimum. Equation (31) also predicts the annihilation cross section to fall at small values of m_χ, dropping to half the maximum value at $m_\chi \simeq 0.25m$. However, in many cases our assumption that $\tilde{l}_R$ exchange dominates the total annihilation cross section is no longer valid in this region.

Going towards smaller values of m_χ, the first prominent structure one encounters is the $t\bar{t}$ threshold. It is most prominent for the dashed curve in Fig. 1(c), since this combination of parameters leads to the smallest value of $|\mu|$; for a given value of M, a smaller $|\mu|$ means larger Higgsino admixtures to the LSP [see Eq. (6a)] and hence larger couplings to h and Z bosons. For most of cases shown in Figs. 1 the contribution of the $t\bar{t}$ final state is suppressed by destructive interference between $\tilde{t}$ and Z exchange contributions, which have approximately equal magnitude but opposite signs here. On the other hand, top-quark production is not p-wave suppressed unless $m_\chi^2 \gg m_t^2$, unlike the production of massless fermions.

FIG. 1. The rescaled LSP relic density Ωh^2 as a function of the LSP mass m_χ for scalar SUSY-breaking mass parameter $m=300$ GeV and four combinations of the ratio $\tan\beta$ of Higgs VEV's and the mass m_t of the top quark. The solid (dashed) curves are for positive (negative) gaugino mass parameter M. Notice that M, the trilinear soft breaking parameter A and the supersymmetric Higgs-boson (Higgsino) mass parameter μ all vary along the curves, due to the relations between model parameters implied by radiative gauge symmetry breaking; in particular, the locations of the pole and thresholds caused by the light scalar Higgs boson are different in each case.

The importance of the $t\bar{t}$ final state compared to light fermions is therefore enhanced by a relative factor $x_F/3 \simeq 10$ [see Eq. (3)].

In the region below the $t\bar{t}$ threshold the differences between the various curves start to become more pronounced. Many of these differences can be understood from Eqs. (27) and (28), which show that increasing m_t and decreasing $\tan\beta$ both imply larger values of μ, which leads to smaller couplings of the LSP to Higgs and gauge bosons, and suppresses contributions from the t-channel exchange of Higgsino-like, heavier neutralinos. This explains why the WW and ZZ thresholds, as well as the minima at $m_\chi = M_Z/2$ and at $m_\chi = m_h/2$, are more prominent in Fig. 1(a) than in 1(b), and why Ωh^2 at small m_χ, where Z exchange diagrams dominate the annihilation cross section, is considerably smaller in Figs. 1(c) and 1(d) than in 1(a) and 1(b). Moreover, m_h increases with increasing m_t and increasing $|\tan\beta|$, so that the position of the h pole tends to move to larger values of m_χ as we go from Fig. 1(a) to 1(d).

The depth and width of the minimum at $m_\chi = m_h/2$ depends quite sensitively on the choice of parameters. Equation (25) shows that in Figs. 1 we always have $m_P^2 \gg M_Z^2$; in this limit the $h\chi\chi$ coupling [42] becomes for a b-ino-like LSP:

$$g_{h\chi\chi} = \frac{g'}{2}\frac{M_Z \sin\theta_W (M_1 + \mu \sin 2\beta)}{M_1^2 - \mu^2} + O\left[\frac{M_Z^2}{M_1^2-\mu^2}, \frac{M_Z^2}{m_P^2}\right]. \quad (32)$$

Notice that the two terms in the numerator tend to cancel if $M_1 \mu \tan\beta < 0$; this explains why the minimum at $m_\chi = m_h/2$ is narrower and shallower for the dashed curves in Figs. 1 than for the solid ones. However, we remind the reader that estimating Ωh^2 from Eqs. (1) to (3) can lead to large errors in the vicinity of a very narrow pole. A more careful treatment [37] would lead to shallower minima, which are broadened in the region below $m_h/2$; if $m_h > M_Z$, the relative maximum between the two minima should therefore also be somewhat lower than indicated in Figs. 1. On the other hand, the h pole clearly affects only a very limited region of parameter space; our overall conclusions do therefore not depend on an accurate treatment of this pole.

Finally, the strength of the $Z\chi\chi$ coupling also depends quite sensitively on the choice of parameters, including their signs. In this case the ordering of the curves for $M > 0$ and $M < 0$ even depends on $\tan\beta$. For $\tan\beta = 2$, a cancellation occurs [43,44] in the neutralino (and chargino) mass matrix if $M_1 \mu \tan\beta > 0$; the LSP then has substantial Higgsino components if $m_\chi \leq M_Z/2$. In contrast, for small $\tan\beta$ and $M_1 \mu \tan\beta < 0$ the LSP remains dominantly a gaugino even if m_χ is very small. On the other hand, for $M < 0$, $\tan\beta = 15$, $\mu(Q_0)$ is quite small due to a strong cancellation in the right-hand side (RHS) of Eq. (27), especially for $m_t = 130$ GeV [Fig. 1(c)]. At larger $|M|$, i.e., larger m_χ, this cancellation is less complete, but for this choice of parameters χ remains dominantly a Higgsino for $m_\chi \leq 60$ GeV, and reaches 90% b-ino content only for $m_\chi \geq 120$ GeV; for $M > 0$ and the same values of m_t and $\tan\beta$, the LSP has already 97% b-ino content at this mass. This explains why the two curves in Fig. 1(c) differ quite strongly even at rather large values of m_χ.

The strong dependence of some of the annihilation cross sections on the model parameters is further illustrated by Fig. 2, which shows a blowup (on a linear scale) of the VV and Zh threshold region for two of the curves of Figs. 1. Both curves show small shoulders at the WW and ZZ thresholds. As explained above, these thresholds are somewhat less pronounced for the case $m_t = 160$ GeV, due to the larger value of μ. However, since for fixed m_χ, μ only increases by approximately 25% as m_t is increased from 130 to 160 GeV, this effect is not very large; see also Eq. (13). This rather small change of parameters suffices, however, to reduce the $\chi\chi \to hh$ cross section by as much as a factor of 6. For $m_t = 130$ GeV, the exchange of the lighter, gauginolike and heavier, Higgsino-like neutralinos gives contributions of approximately equal size and equal sign to the matrix element. In other words, the terms $\propto d_8$ and $\propto d_9$ in Eq. (17) have about equal magnitude here; notice that the larger SU(2) gauge coupling can only enter via d_9 in case of a b-ino-like LSP. Going to larger m_t does not only increase μ for fixed M, it also increases m_h via the radiative correction Δ_{22} of Eq. (26); this necessitates an increase of M, and thus a further increase of μ, in order to reach the hh threshold. The contributions $\propto d_9$ are therefore almost negligible for the dashed curve in Fig. 2. Indeed, the decrease of this curve after the maximum at $m_\chi = 62$ GeV has nothing to do with any thresholds; rather it is caused by the increase of the slepton exchange contribution to the l^+l^- final state [see Eq. (31)]. Finally, we remind the reader that a cancellation occurs in the contribution to the hh final state from Higgsino exchange if $M_1 \mu \tan\beta < 0$ [see Eq. (18)];

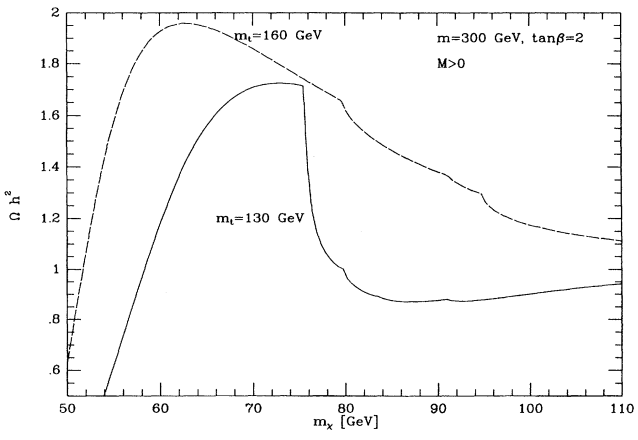

FIG. 2. An enlargement of the threshold region of the solid curves in Figs. 1(a) and 1(b). For $m_t = 130$ GeV (solid curve) the hh and Zh final states are accessible for $m_\chi > 75$ and 84 GeV, respectively, while for $m_t = 160$ GeV (dashed), they are only accessible for $m_\chi > 95$ and 93 GeV, respectively.

this contribution is also suppressed for large $\tan\beta$ if $|\mu| \gg |M_1|$. The hh threshold is therefore all but invisible in most curves in Figs. 1.

It has been noted in Ref. [37] that our estimate of Ωh^2, Eqs. (1)–(3), becomes unreliable in the vicinity of a threshold for a final state which quickly dominates the total annihilation cross section. The example given there was exactly the hh final state, which for certain combinations of parameters can dominate the total cross section by a large factor. However, we find that such a situation never occurs for b-ino-like or mixed LSP's in minimal SUGRA; in this case the hh threshold, as well as all other thresholds, is never much more pronounced than for the solid curve in Fig. 2, and usually the thresholds are much less important, as can be seen from Figs. 1. We do therefore not expect the error introduced by our approximate treatment to exceed 10% just below threshold, and it should be much smaller everywhere else.

So far we have concentrated on examples where the LSP is dominantly a b-ino, the exception being the dashed curve in Fig. 1(c). Since the LSP will only be Higgsino-like if $|\mu| < |M_1| \simeq 0.43|M|$, one obviously needs quite large values of $|M|$ to get a Higgsino-like LSP with mass substantially above M_Z. The SUGRA constraints then imply that one also needs large m, since for $M^2 \gg m^2$ Eqs. (27) and (28) always yield $|\mu| \geq |M_1|$ for experimentally allowed values of m_t. In Fig. 3 we have therefore chosen $m=2$ TeV, and present results for two different choices of M and m_t. In this figure, μ, A, and $\tan\beta$ all vary along the x axis, with $m_\chi \simeq |\mu|$. As in Figs. 1, we see that Ωh^2 is essentially independent of most parameters if the LSP is a heavy, almost pure state, here an almost pure Higgsino. Of course, once $|\mu| > |M_1|$ the LSP will become b-ino-like again, and will thus have a very small annihilation cross section, since the very large m implies very heavy sfermions; this explains the steep rise of the dashed curve at $m_\chi \simeq 430$ GeV.

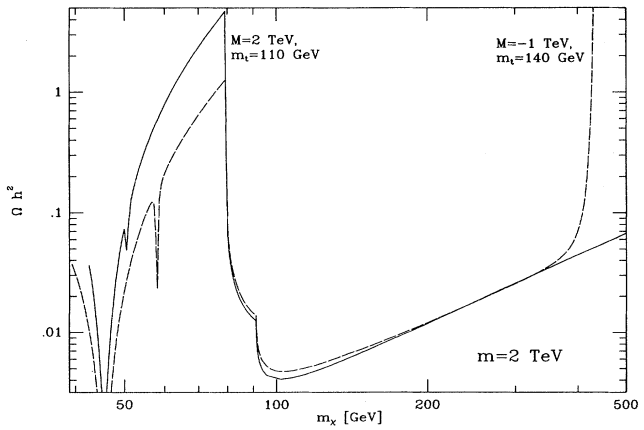

FIG. 3. The rescaled LSP density as a function of the LSP mass for two examples of Higgsino-like LSP's. M, m, and m_t are fixed for each curve, while μ, A, and $\tan\beta$ vary. For $M=-1$ TeV (dashed curve) the LSP becomes b-ino-like at $m_\chi \simeq 430$ GeV, which explains the rapid rise of this curve at large m_χ. Only $\chi\chi$ annihilation has been included in the calculation; this substantially overestimates Ωh^2 for $m_\chi \leq M_W$, as argued in the text.

Notice that this curve does not have a relative minimum in the region $|\mu| \simeq |M_1|$, even though here both the Higgsino and gaugino components of the LSP are large; this seems to be in conflict with results of Refs. [18,26]. However, in our case Eq. (25) implies that all Higgs bosons except h are very heavy, so that most final states containing Higgs bosons are not accessible; moreover, contributions from P exchange in the s channel are suppressed, even though the $P\chi\chi$ coupling is large for a mixed LSP. The $\chi\chi \to f\bar{f}$ cross section does show a maximum in the region where χ is a mixed state, due to the contributions from Z and h exchange, but this is not sufficient to compensate the rapid decrease of the VV and Zh cross sections.

For $m_\chi < M_W$ the annihilation of Higgsino-like LSP's is dominated by Z-exchange diagrams. Equations (10) and (7) show that $g_{Z\chi\chi} \propto M_Z^2/(\mu M_1)$ in this case; the $\chi\chi$ annihilation cross section is therefore about 4 times smaller for $M=2$ TeV than for $M=-1$ TeV. However, the results of Fig. 3 are quite misleading in this region. We had already mentioned above that Eqs. (1)–(3) are not valid [37] close to a threshold where a new channel opens up which quickly dominates the total annihilation cross section, as is the case for the WW threshold here; this is because we ignored the possibility that LSP's with mass below M_W can annihilate into WW pairs if they have sufficient kinetic energy. Therefore we have overestimated the relic density in the region just below and at the WW threshold.

Moreover, as already discussed in Sec. II B, a light Higgsino-like LSP always implies the existence of a second Higgsino-like state χ' whose mass is quite close to that of the LSP. Since the $Z\chi\chi'$ coupling is *not* suppressed, unlike the $Z\chi\chi$ coupling, the $\chi\chi'$ coannihilation cross section is much larger than $\sigma_{\text{ann}}(\chi\chi)$ [see Eq. (12)]. Furthermore, $\chi\chi'$ coannihilation is *not* p-wave suppressed even if the final-state fermions are massless. Using the formalism of Ref. [37], we estimate that inclusion of $\chi\chi'$ coannihilation would reduce Ωh^2 by a factor

$$K \simeq \left[1+\frac{x_F}{3}\frac{2}{\epsilon^2}e^{-x_F\Delta}\right] \Big/ (1+e^{-x_F\Delta})^2 . \tag{33}$$

Here $\Delta \equiv |(|m_3|-|m_4|)/\mu|$ is given by Eq. (8) and ϵ by Eq. (7). The exponential factor describes the Boltzmann suppression of the χ' density at freeze-out; we find $x_F \simeq 25$ in this case. The factor of $x_F/3$ in front of the second term in the numerator of Eq. (33) has been included to estimate the s-wave enhancement (or, more accurately, lack of p-wave suppression) to the coannihilation process, and the 2 is a statistics factor [37]. Numerically we find $K \simeq 4$ (80) for $|M|=1$ TeV and $|\mu|=50$ (80) GeV; for $|M|=2$ TeV the corresponding numbers are 230 and 1500, respectively. Of course, these estimates could easily be off by a factor of 2 or so; nevertheless, taken together with subthreshold $\chi\chi$ annihilation into W pairs, these large suppression factors allow us to conclude that the relic density of Higgsino-like LSP's will always be uninterest-

ingly small unless $m_\chi \geq 500$ GeV or so.[14]

We had seen in Figs. 1 that over a wide region of parameter space the relic density of a heavy, b-ino-like LSP depends only very little on m_t, $\tan\beta$ and the sign of M. However, as already pointed out in Ref. [32], this is no longer true for very large values of $|\tan\beta|$. This is illustrated in Fig. 4, where we show Ωh^2 as a function of $\tan\beta$ for fixed m, M, and m_t; the parameters are chosen such that χ is b-ino-like. The solid line shows the SUGRA prediction including the contributions from the b and τ Yukawa couplings to the neutralino-fermion-sfermion interactions as well as to the RGE. These latter contributions reduce m_P, as shown in Eq. (25); they also reduce the masses of the lighter $\tilde{b}$ and $\tilde{\tau}$ eigenstates by mixing between SU(2)-singlet and -doublet states, and by reducing the diagonal entries of their mass matrices.

Figure 4 shows that both these effects are quite important. When $\tan\beta$ is increased sufficiently, one eventually has $m_P = 2m_\chi$; for the parameters of Fig. 4 this happens as $\tan\beta \simeq 35$. This results in a very strong enhancement of the $\chi\chi \to b\bar{b}$, $\tau^+\tau^-$ cross sections via the exchange of a pseudoscalar Higgs boson. Note that the $Pb\bar{b}$ and $P\tau^+\tau^-$ couplings increase $\propto \tan\beta$, so that the total decay width $\Gamma_P \propto \tan^2\beta$. For $\tan\beta = 35$ the mass-to-width ratio of P is therefore similar to that of the Z boson, so that our estimate of Ωh^2 should be quite reliable even in the pole region [37].

The long dashed curve has been obtained by artificially keeping m_P constant at the value SUGRA predicts for $\tan\beta = 2$ ($\simeq 780$ GeV); this also implies that m_{H^+} and m_H are kept (approximately) constant. However, the $\tilde{b}$ and $\tilde{\tau}$ masses are still allowed to vary with $\tan\beta$ as predicted by SUGRA, and the Yukawa contributions to the neutralino couplings are included; we see that this suffices to reduce Ωh^2 by approximately a factor of 3 at the largest allowed value of $\tan\beta$. The reduction of $m_{\tilde{\tau}_1}$ is the dominant effect here, since for the given choice of m and M the $\tilde{b}$ squarks are almost twice as heavy as the $\tilde{\tau}$ sleptons, and have smaller hypercharge. Because for the given choice of parameters one has $m_\chi^2 \ll m_{\tilde{f}}^2$, the annihilation cross section is essentially proportional to $\sum_i Y_i^4/m_{\tilde{f}_i}^4$ here, where i is a generation index; at small $\tan\beta$, all three generations contribute almost equally, but for large $\tan\beta$ the sum is dominated by the contribution from the third generation. The reduction of Ωh^2 by a factor of 3 then corresponds to a reduction of $m_{\tilde{\tau}_1}$ by only a factor of 1.63. An even larger reduction of the $\tilde{\tau}$ mass is not possible here

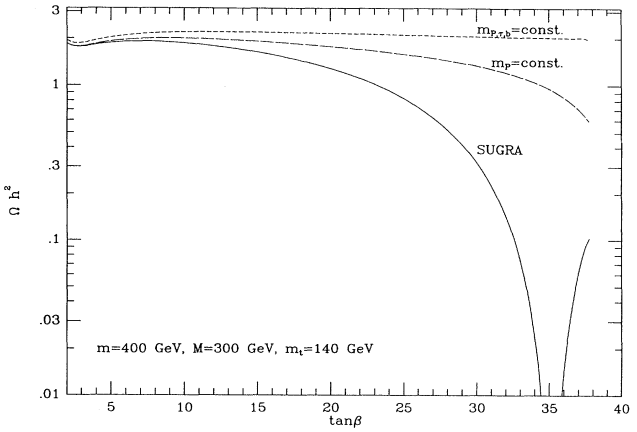

FIG. 4. Demonstration of the importance of the SUGRA imposed relations between particle masses. The solid curve shows the full SUGRA prediction for Ωh^2 as a function of $\tan\beta$; Eq. (25) implies that $m_\chi = m_P/2$ at $\tan\beta = 35.3$, where P denotes the pseudoscalar Higgs boson. The long dashed curve has been obtained by keeping m_P constant at the value SUGRA predicts for $\tan\beta = 2$, i.e., $m_P = 783$ GeV, but the $\tilde{\tau}$ and $\tilde{b}$ masses are still allowed to vary with $\tan\beta$. For the short dashed curve all effects of the b and τ Yukawa couplings have been switched off.

since a further increase of $\tan\beta$ would lead to $m_P^2 < 0$; as shown in Ref. [32], this constraint implies $|\tan\beta| \leq m_t(Q_0)/m_b(Q_0)$. Finally, the short dashed curve has been obtained by ignoring all effects from the b and τ Yukawa couplings; it is a few percent above the other curves even at small $\tan\beta$ since the effects of sfermion mixing are not entirely negligible even here. We see that in this case, which approximates the usual analyses based on a global SUSY model with independent sparticle masses at the weak scale, Ωh^2 does indeed only depend very little on $\tan\beta$.

Using the insight gained from Figs. 1–4 it is now quite straightforward to interpret the contour plots of Figs. 5 and 6. Each of these figures is for fixed values of m and m_t and for a given choice of the signs of M and $\tan\beta$. In Figs. 5(a)–5(d) we choose $m = 250$ GeV, $m_t = 140$ GeV, and explore the plane of M and $\tan\beta$ for all four combinations of signs. Solid and long dashed lines are contours of constant $\Omega h^2 = 1$ and 0.25, respectively. The short dashed curves in Fig. 5(a) are lines of constant $\Omega h^2 = 0.025$; since these contours cluster very narrowly around the Z, h, and P poles, in the other figures we have merely indicated the position of these poles with the short dashed lines.

Finally, the region outside the dotted curves is excluded by the experimental and theoretical constraints discussed at the end of Sec. II C. In the region of small $|M|$ the most important constraints are the LEP search limits (29a)–(29d) as well as the gluino mass bound (29f); for small $|\tan\beta|$ the LEP limit on the production of the light scalar Higgs boson also plays a role. The lower bound on $|\tan\beta|$ is determined by the Higgs-boson search bound as well as the requirement that the Higgs potential should be bounded from below even at the GUT scale, as discussed

[14]Of course, coannihilation will also occur for $m_\chi > M_W$; indeed, the relative mass splitting Δ between the Higgsino states, and hence the Boltzmann suppression of the coannihilation contribution, will be (much) smaller than for light Higgsinos. On the other hand, $\sigma_{\rm ann}(\chi\chi')$ should not be much bigger than $\sigma_{\rm ann}(\chi\chi)$ in this case, since $\sigma_{\rm ann}(\chi\chi)$ is dominated by annihilation into a pair of gauge bosons, which occurs with full gauge strength; in the region $m_\chi > M_W$ coannihilation should therefore not change the result of Fig. 3 much.

in Sec. II C below Eq. (30). The region of large $|\tan\beta|$ and small and moderate values of $|M|$ is limited by the LEP bounds on associate hP production, which is practically equivalent to requiring $m_P^2 > 0$ here, since the overall mass scale (m) is chosen quite high in these figures. Finally, in the region of large $|M|$ (or, more accurately, large $|M/m|$) the parameter space is limited by the requirement of a neutral LSP, Eq. (29f); this bound is especially important for large $|\tan\beta|$, since $m_{\tilde{\tau}_1}$ is smaller there, as discussed in connection with Fig. 4.

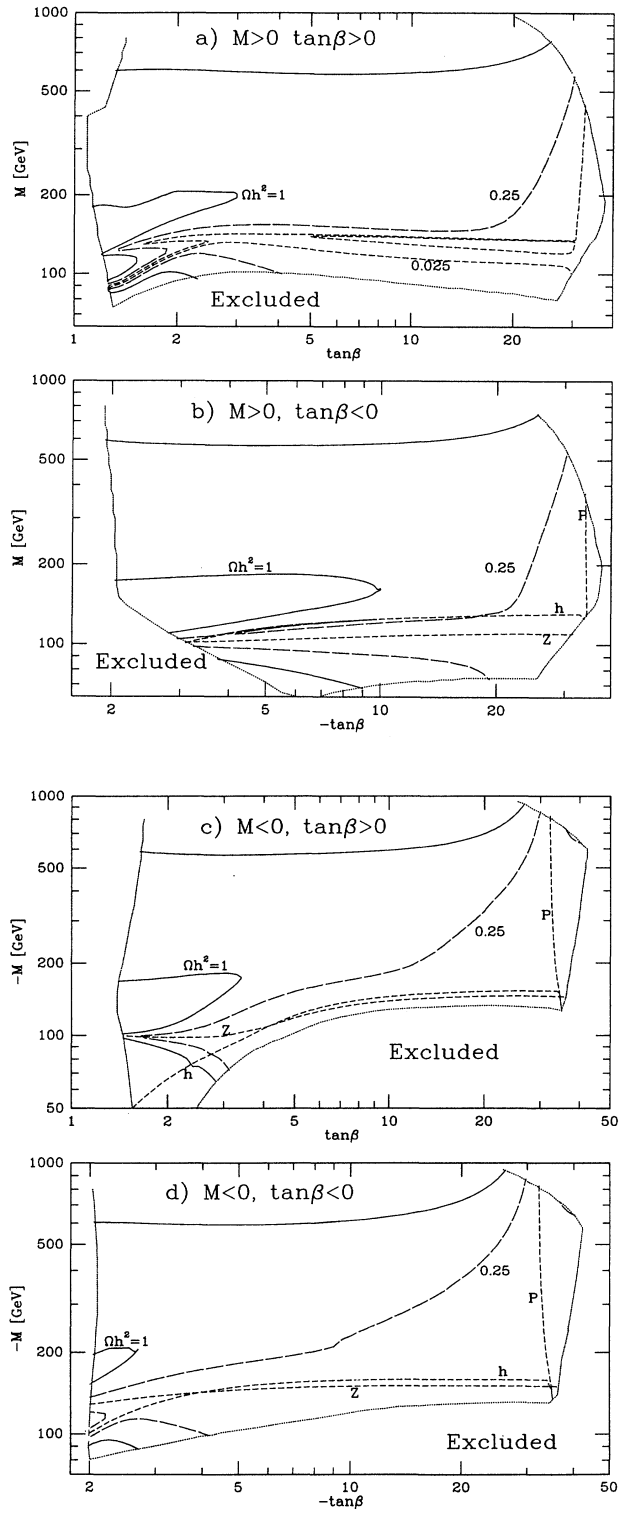

The gross features are the same in all four figures. At large $|M|$, Ωh^2 exceeds 1, as already shown in Figs. 1; this also happens at small $|\tan\beta|$ and small $|M|$, below the Z and h poles. Finally, there is a third region where the χ relic density is unacceptably large, covering the region between the Z and h poles and the VV, Zh, and hh thresholds at small and moderate values of $|\tan\beta|$. The extension of these last two excluded regions does depend on the signs of M and $\tan\beta$, however. We have already seen that the contribution from h exchange and the annihilation cross section into the hh final state are much smaller if $M_1\mu\tan\beta < 0$ [Figs. 5(b) and 5(c)]; in this case the line $\Omega h^2 = 0.25$ can even cross the h pole. Moreover, for $|M| \leq 300$ GeV negative values of $\tan\beta$ [Figs. 5(b) and 5(d)] require rather large, positive values of A; if in addition $M > 0$, X_2 of Eq. (28) and hence $|\mu|$ become large, leading to small Higgsino components of the LSP and thus large values of Ωh^2 in Fig. 5(b). In Fig. 5(d) we have $M < 0$, however, which results in a partial cancellation in X_2 and much smaller values of $|\mu|$; together with sizable contributions from h exchange and hh production this explains the smallness of the cosmologically excluded region for this choice of signs. On the other hand, small or moderately positive values of $\tan\beta$ imply $A \simeq 0.5$ in the region $|M| \leq m$, reducing the impact of this parameter on X_2 and μ; furthermore, choosing $M > 0$ now results in larger contributions from the light Higgs boson. The differences between Figs. 5(a) and 5(c) in the experimentally allowed region are therefore smaller than those between Figs. 5(b) and 5(d).

Because of the cancellation in the neutralino mass matrix discussed in connection with Figs. 1, LEP constraints from neutralino searches lead to a more stringent limit on $|M|$ if $M_1\mu\tan\beta > 0$; this explains why the experimentally allowed, but cosmologically excluded region of small $|M|$ is larger in Figs. 5(b) and 5(c) than in 5(a) and 5(d). Finally, as shown in Ref. [32], one can only achieve $|\tan\beta| \gg 1$ for sizable values of μ if $A > 0$, and usually $A > m$; choosing $M < 0$ then reduces the effect of the Yukawa coupling on the running of scalar masses, as exemplified by X_2, Eq. (28). Somewhat paradoxically, this reduces m_P, because in the relevant limit $\tan^2\beta \gg 1$ Eqs. (25) and (27) imply

FIG. 5. Contours of constant Ωh^2 in the plane spanned by M and $\tan\beta$, for fixed $m = 250$ GeV and $m_t = 140$ GeV; results for all four combinations of signs of M and $\tan\beta$ are shown. The solid and long dashed lines are contours where $\Omega h^2 = 1$ and 0.25, respectively. The short dashed lines in (a) are contours where $\Omega h^2 = 0.025$; since these contours are very close to the Z, h, or P poles, in (b)–(d) we have merely indicated the location of these poles by the short dashed lines. The region outside of the dotted curves is excluded by various experimental and theoretical constraints, as described in the text. A flat universe requires $0.25 \leq \Omega h^2 \leq 1$, while LSP's can build up the dark-matter halo of galaxies if $\Omega h^2 \geq 0.025$.

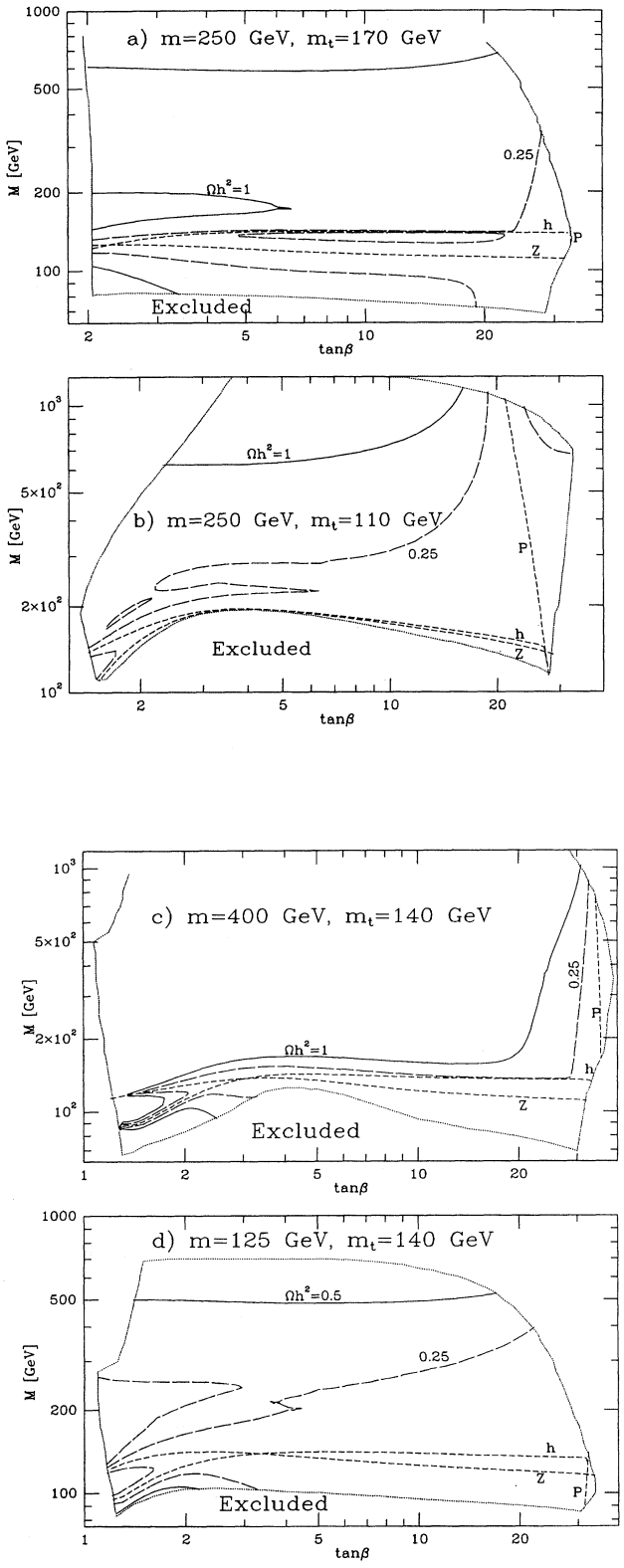

FIG. 6. Contours of constant Ωh^2 in the plane spanned by M and $\tan\beta$, for the quadrant $M>0$, $\tan\beta>0$, and four different combinations of m and m_t as indicated. The notation is as in Figs. 5(b)–(d).

$m_P^2 \propto X_2$. A smaller X_2 also implies smaller μ and hence less τ-slepton mixing, which again increases $m_{\tilde{\tau}_1}$. Altogether we thus see that choosing $M<0$ leads to smaller values of m_P and larger $m_{\tilde{\tau}_1}$ in the region of large $|\tan\beta|$. The region of parameter space to the right of the P pole that is allowed by the requirement $m_\chi \le m_{\tilde{\tau}_1}$ is therefore somewhat larger for $M<0$ [Figs. 5(c) and 5(d)] than for $M>0$ [Figs. 5(a) and 5(b)]. One even finds another small region with $\Omega h^2>0.25$ at very large $|\tan\beta|$ and $M\simeq -800$ GeV.

In Figs. 6 we have chosen M and $\tan\beta$ to be positive, and study the effects of varying m_t [Figs. 6(a) and 6(b)] or m [Figs. 6(c) and 6(d)]. We have already seen that increasing m_t increases $|\mu|$, and thus also Ωh^2 if χ is b-inolike. Indeed we find larger cosmologically excluded regions in Fig. 6(a) than in Fig. 5(a). Moreover, the fraction of the plane with $M<200$ GeV where $\Omega h^2>0.25$ is now much larger than before. This is partly due to the increase of the mass of the light Higgs boson caused by the increase of Δ_{22} in Eq. (26). For $\tan\beta\ge 5$ the h and Z poles are now sufficiently far apart to allow for a new region with cosmologically interesting DM density in between these poles. Larger values of $|\mu|$ also imply [32] more $\tilde{\tau}$ mixing, which reduces $m_{\tilde{\tau}_1}$; at the same time increasing $|\mu|$ implies larger values of m_P [see Eq. (25)]. The neutral LSP constraint (29f) therefore does no longer allow to choose $|\tan\beta|$ so large that $m_P\simeq 2m_\chi$, except for a small stretch at $M\simeq 130$ GeV; the effect of the reduction of m_P and $m_{\tilde{\tau}_1}$ at large $\tan\beta$ is nevertheless still quite pronounced in Fig. 6(a). Finally we mention that the requirement that the top Yukawa coupling remains finite up to scale M_X implies $|\tan\beta|\ge 2$ for $m_t=170$ GeV.

Reducing m_t from 140 to 110 GeV [Fig. 6(b)], has obviously the opposite effect as increasing it to 170 GeV. $|\mu|$ is now so small that the whole region of small and moderate $|M|$ is cosmologically safe; however, this also implies larger couplings of the lighter neutralino states to the Z boson, so that the LEP search limits rule out a much larger part of the plane than in Fig. 5(a). (Recall that the signs of the parameters are such that cancellations occur in the determinant of the neutralino mass matrix.) We already saw in Fig. 2 that the hh contribution depends very sensitively on M, μ, and $\tan\beta$; in the given case it is large enough to create a small "island" with $\Omega h^2<0.25$ at $\tan\beta\simeq 2$, $M\simeq 200$ GeV. Moreover, for given values of M and $\tan\beta$, $m_{\tilde{\tau}_1}$ is now larger and m_P is smaller than in Fig. 5(a), so that a sizable region of parameter space to the right of the P pole is again allowed, including a substantial region where $\Omega h^2>0.25$. The relatively light pseudoscalar here even affects the cosmologically excluded region at very large M, leading to a much steeper slope of the uppermost solid line than in Fig. 5(a). Finally, the reduction of $|\mu|$ also implies that the requirement (30) of a bounded Higgs potential at scale M_X now excludes a large region of parameter space at large $|M|$ and small $\tan\beta$.

In Figs. 6(c) and 6(d) we have again chosen $m_t=140$ GeV, but have varied m compared to the value of Fig.

5(a). A larger m means larger sfermion masses and hence smaller contributions from sfermion exchange diagrams, which are dominant at large $|M|$, as we have seen above. Indeed, we see that the uppermost contour with $\Omega h^2=1$, which (at least for small $|\tan\beta|$) occurred essentially in the same place in the previous six figures, depends very strongly on m: For $m=400$ GeV the cosmologically safe region above the VV, Zh, and hh thresholds has disappeared completely; on the other hand, for $m=125$ GeV [Fig. 6(d)], all experimentally allowed combinations of M and $\tan\beta$ give $\Omega h^2<1$, so that the requirement that the relic LSP density should not overclose the Universe does not constrain the parameter space any further. Recall that an increase of m also implies an increase of $|\mu|$ via Eq. (27); this explains the differences in the region of small M, below and around the h pole, between Figs. 5(a), 6(c), and 6(d), even though sfermion exchange contributions are essentially negligible here. Finally, for $m=125$ GeV we observe a region with very small relic density, $\Omega h^2<0.25$, in approximately the same place that leads to $\Omega h^2>1$ for $m=250$ GeV; this once again demonstrates the strong dependence of the contributions from gauge and Higgs final states on the parameters of the model.

This concludes our discussion of samples of the parameter space of the model. We now attempt to derive bounds on sparticle masses or model parameters from computations of the DM density.

IV. BOUNDS

We have seen in the previous section that very heavy LSP's tend to have small annihilation cross sections. This is not surprising, since unitarity requires the cross section to fall off at least like $1/m_\chi^2$ as $m_\chi\to\infty$, for fixed values of the other parameters. Indeed, we see from Figs. 5 that for given m and m_t the requirement $\Omega h^2\le 1$ imposes an upper bound on $|M|$. Moreover, in the important case of a b-ino-like LSP away from all (Z and Higgs) poles, the resulting bound depends essentially only on m and m_χ, as shown in Figs. 1, 5, and 6. The SUGRA relations for sfermion masses (22) imply that the sfermions with the largest hypercharge, the superpartners $\tilde{l}_R$ of the right-handed leptons, also have the smallest masses; they will therefore dominate the annihilation cross section unless $M^2\ll m^2$, as already pointed out in the previous section. From Eqs. (22) and (31) and the numerical result of Figs. 1 that $\Omega h^2\simeq 1$ for $m=300$ GeV, $m_\chi=180$ GeV if χ is b-ino-like, one then derives the approximate bound

$$\frac{(m^2+1.83m_\chi^2)^2}{m_\chi^2\left\{\left[1-\frac{m_\chi^2}{(m^2+1.83m_\chi^2)}\right]^2+\left[\frac{m_\chi^2}{(m^2+1.83m_\chi^2)}\right]^2\right\}}\le 1\times 10^6\ \text{GeV}^2\ ; \quad (34)$$

this bound is only valid for a b-ino-like LSP away from poles. We already mentioned in the previous section that for fixed m the LHS of (34) has a minimum at $m_\chi=0.6m$. Plugging this into the bound (34) gives

$$m\le 300\ \text{GeV} \quad (35)$$

for any value of m_χ; this can also be read off Figs. 1. Similarly, for given m_χ the LHS of (34) is minimized by choosing m as small as allowed by the constraint $m_{\tilde{l}_R}\ge m_\chi$, i.e., for $m^2+0.83m_\chi^2=m_\chi^2$. This immediately gives the bounds

$$m_\chi\le 350\ \text{GeV}\ , \quad (36a)$$

$$|M|\le 825\ \text{GeV}\ , \quad (36b)$$

for any m. The bound (36a) is considerably stronger than the bound of 550 GeV given in Ref. [18], because in that paper *all* sfermions were allowed to have mass $m_{\tilde{f}}=m_\chi$, which is not possible in minimal SUGRA. In particular, a light top squark greatly enhances the annihilation into $t\bar{t}$ pairs, which also makes a sizable contribution to the s-wave, $O(v^0)$ cross section.

We emphasize again that the bounds (34)–(36) only hold for a b-ino-like LSP away from poles. In particular, the bound (35) on m can be violated even for small $|\tan\beta|$ if m_χ is close to $M_Z/2$ or $m_h/2$ [see Fig. 6(c)]; in this case no useful bound on m can be given. Moreover, Figs. 5 and 6 show that for a given combination of m, m_t, and $\tan\beta$, the upper bound on $|M|$ is weakest in the region close to the P pole, if $m\ge 150$ GeV. More precisely, $|M|$ reaches its maximal allowed value at the point where the contour for $\Omega h^2=1$ (which has a positive slope with increasing $|\tan\beta|$) meets the line $m_{\tilde{\tau}_1}=m_\chi$ (which has a negative slope). The situation of this crossing point obviously depends on how large $m_{\tilde{\tau}_1}$, m_P, and the $P\chi\chi$ coupling $g_{P\chi\chi}$ are for a given choice of M and $\tan\beta$. We have already mentioned in the previous section that both $|\mu|$ and m_P grow with increasing X_2 [Eq. (28)]. Moreover, choices of parameters that maximize X_2 also maximize the reduction of the diagonal elements of the $\tilde{\tau}$ mass matrix due to the effect of the τ Yukawa coupling on the RGE. Finally, increasing $|\mu|$ further reduces $m_{\tilde{\tau}_1}$ by increasing $\tilde{\tau}_L$-$\tilde{\tau}_R$ mixing, and reduces $g_{P\chi\chi}$ by reducing the Higgsino component of χ [see Eq. (6a)]. Combinations of parameters that increase X_2 therefore push the P pole to larger values of $|\tan\beta|$, and also make it narrower and shallower; at the same time they strengthen the upper bound on $|\tan\beta|$ that results from the requirement $m_{\tilde{\tau}_1}\ge m_\chi$. The combined effect of these changes is to move the crossing point of the lines $m_{\tilde{\tau}_1}=m_\chi$ and $\Omega h^2=1$ to smaller $|M|$ and smaller $|\tan\beta|$.

We already discussed in connection with Figs. 5 that in the region of large $|\tan\beta|$ one has $A>0$, so that X_2 is smaller for $M<0$ than for $M>0$. The absolute bound on $|M|$ for given m and m_t is therefore reached if M and $\tan\beta$ are both negative [see Fig. 5(d)]. The resulting upper bound on $|M|$ as a function of m is shown in Fig. 7 for three different choices of m_t. For $m\le 125$ GeV the upper bound on $|M|$ only comes from the requirement $m_{\tilde{\tau}_1}\ge m_\chi$; for these small values of m the constraint (34) is satisfied even for the extreme case $m_\chi=m_{\tilde{l}_R}$. Here the maximal allowed $|M|$ occurs at rather small values of $|\tan\beta|$, where $m_{\tilde{\tau}_1}\simeq m_{\tilde{\tau}_R}$ only depends on m and M; for small m the bound on $|M|$ is therefore almost independent of m_t. However, once the condition $\Omega h^2\le 1$ starts

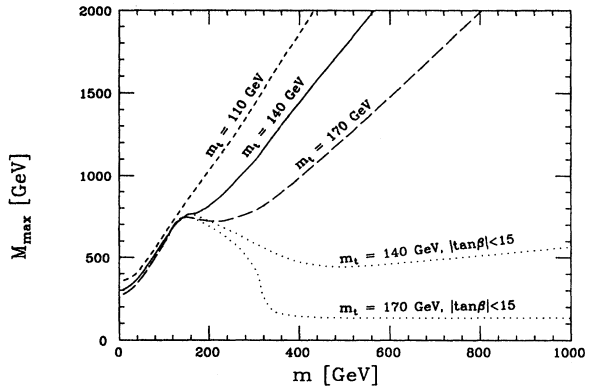

FIG. 7. The upper bound on $|M|$ which follows from the requirement that LSP's do not overclose the universe, $\Omega h^2 \leq 1$. The long dashed, solid, and short dashed curves are valid for $m_t = 110$, 140, and 170 GeV, respectively, and show the absolute upper bound over the entire experimentally and theoretically allowed parameter space. The dotted curves emerge when one restricts the parameter space to $|\tan\beta| \leq 15$; the upper (lower) dotted curve is for $m_t = 140$ (170) GeV. In all cases the maximal $|M|$ is found in the quadrant $M < 0$, $\tan\beta < 0$.

to impose nontrivial constraints on the allowed parameter space, the bound on $|M|$ comes from the region of large $|\tan\beta|$ and does depend quite strongly on m_t. For light top quark and thus small X_2 (short dashed curve), the DM constraint reduces $|M|_{max}$ only marginally from the value of $5.7m$ that follows from the simple requirement $m_{\tilde{l}_R} > m_\chi$. On the other hand, if the top quark is very heavy (long dashed curve), a relatively large ratio $|m/M|$ is needed to get sufficiently close to the P pole without reducing $m_{\tilde{\tau}_1}$ below m_χ. Finally, $|M|_{max}$ also depends quite sensitively on the chosen combination of signs; for instance, if M and $\tan\beta$ are both positive one finds $M < 2150(1210, 620)$ GeV for $m = 500$ GeV and $m_t = 110(140, 170)$ GeV, respectively.

The rise of the curves in Fig. 7 cannot persist indefinitely. Right on the pole, for $m_\chi = m_P/2$, the annihilation cross section is proportional to $g^2_{P\chi\chi}/\Gamma^2_P$. The decay width Γ_P is proportional to m_P, and thus also to m_χ; moreover, the $P\chi\chi$ coupling decreases $\propto 1/m_\chi$ if χ is b-ino-like [see Eq. (6a)]. As a result, the annihilation cross section for a b-ino-like LSP on the P pole decreases $\propto 1/m_\chi^4$. We estimate that Ωh^2 will be larger than 1 even right on the pole if $m_\chi \geq 3.5$ (1.7) TeV for $m_t = 140$ (170) GeV. If the top quark is lighter, one can arrange $m_\chi = m_P/2$ even for a mixed LSP, i.e., if $|M_1| \simeq |\mu|$. In this case $g_{P\chi\chi}$ is not suppressed by small mixing angles, which increases the cross section by a factor $(m_\chi/M_Z)^2$ compared to the case of a b-ino-like LSP. The relic density of a mixed LSP with $m_\chi = m_P/2$ will therefore only exceed 1 if $m_\chi \gtrsim 100$ TeV or so. One can hardly speak of "weak scale" supersymmetry if the *lightest* superparticle is thousand times heavier than the weak gauge bosons; in particular, the model can no longer provide a solution of the naturalness problem.

It can be argued that fine-tuning is needed to achieve $|\tan\beta| \gg 1$, because this occurs only over a narrow range of values of A. Moreover, in minimal supersymmetric SU(5) the proton decay width increases [58] $\propto \tan^2\beta$, since in this model proton decay is mostly mediated by the exchange of superheavy Higgsinos, whose Yukawa couplings grow $\propto |\tan\beta|$; large values of $|\tan\beta|$ are then disfavored (although "accidental" cancellations might still lead [58] to an acceptable nucleon lifetime even if $|\tan\beta| \gg 1$). Figure 7 therefore also includes curves (dotted) where we have required $|\tan\beta| \leq 15$. This rather mild constraint does not affect the curve for $m_t = 110$ GeV at all, but for a heavier top quark it leads to a substantial reduction of $|M|_{max}$. Since $m_\chi \simeq m_P/2$ is no longer possible in this case, the only possibility to achieve large values of $|M|$ is to choose parameters such that the LSP is Higgsino-like.

We have already seen in Fig. 3 that the relic density of such a state is quite small. By extrapolation of the curves of this figure it is clear that a Higgsino-like LSP is cosmologically safe up to $m_\chi = 2$ TeV at least; this has already been shown in Refs. [18] and [19]. The LSP will obviously only be Higgsino-like if $|M_1| \simeq 0.43|M| \geq |\mu|$, but this requirement might clash with the constraints imposed by radiative gauge symmetry breaking, Eqs. (27) and (28). Clearly $\mu^2(Q_0)$ can be minimized by choosing A such that X_2 is minimal, $A \simeq -2.08M$. For $\tan^2\beta \gg 1$, Eqs. (27) and (28) then give the following lower bound on $|\mu|$:

$$\mu^2(Q_0) \geq m^2\left[0.9\left[\frac{m_t}{150\text{ GeV}}\right]^2 - 1\right] + M^2\left[\left[\frac{m_t}{150\text{ GeV}}\right]^2\left\{2.7 - 1.04\left[1 - \left[\frac{m_t}{190\text{ GeV}}\right]^3\right]\right\} - 0.52\right]. \quad (37)$$

Notice that the coefficient of M^2 is positive for $m_t \geq 85$ GeV; it surpasses $(M_1/M)^2 \simeq 0.18$ for $m_t \geq 95$ GeV, i.e., in almost the entire experimentally allowed region. The condition for having a Higgsino-like LSP, $|\mu(Q_0)| \leq |M_1|$, is therefore most easily satisfied if $|M|$ (and thus $|M_1|$) is itself very small. However, the coefficient of m^2 in Eq. (37) also turns positive for $m_t > 158$ GeV. For such a heavy top quark a Higgsino-like LSP can therefore *not* be realized in minimal SUGRA. For this reason the lower dotted curve in Fig. 7, which is valid for $m_t = 170$ GeV, is essentially just given by the bound (34) in the region where DM constraints are relevant and the condition (35) is satisfied; for $m > 300$ GeV this curve simply follows the h pole, $m_\chi \simeq 0.43|M| \simeq m_h/2$.

For $m_t = 140$ GeV (upper dotted curve) a Higgsino-like LSP is still possible provided $|M/m| \leq 0.5$ or so. The actual bound on $|M|$ is in many cases substantially above this value since for moderately large m the total $\chi\chi$ annihilation cross section is still sufficiently large even if the Higgsino component of χ is subdominant; in particular the contribution from the $t\bar{t}$ final state plays an important role here. However, increasing m decreases the sfermion exchange contribution to the total annihilation cross section; this has to be compensated by increasing the Higgsi-

no content of χ, i.e., by reducing $|\mu/M|$, which via Eq. (37) reduces the bound on $|M/m|$. As a result the bound on the absolute value of $|M|$ is almost independent of m for 400 GeV $\leq m \leq 1$ TeV; for even larger values of m the LSP can be an almost pure Higgsino even for $M > 0.5$ TeV, and one has $|M|_{\max} \simeq 0.6m$. Finally, we mention that a further sharpening of the bound on $|\tan\beta|$, e.g., requiring $|\tan\beta| \leq 5$, would suppress the bound on $|M|$ for $m_t = 140$ GeV to a value very close to the one for $m_t = 170$ GeV. This is because solutions with $\mu^2 \ll m^2$ always have $\tan^2\beta \gg 1$, unless one has $|A| \gg m$; however, Eqs. (27) and (28) show that large $|A/m|$ require $|\mu|$ to be larger than $|M_1|$, unless m_t is near its present lower bound [59] of 91 GeV.

This completes our discussion of possible upper bounds on mass parameters of the model that can be derived from the requirement $\Omega h^2 \leq 1$. What about lower bounds? In principle the bound (34) also implies a lower bound on the mass of a b-ino-like LSP if m is fixed within the region allowed by the limit (35). Recall, however, that these bounds are only valid if χ is a nearly pure b-ino and m_χ is not close to a pole. Both these conditions can be violated quite easily especially if m_χ is not large. Indeed, Figs. 5 and 6 show that for most combinations of m, m_t, and $\tan\beta$ the lower bound on $|M|$ is determined from laboratory search limits alone, the exception being the region of small $|\tan\beta|$ and $m > 200$ GeV. In particular, inclusion of the DM constraint does not strengthen the bound $m_\chi > 20$ GeV that follows [48] from the combination of the gluino, chargino and neutralino search limits.

On the other hand, we have seen in Fig. 6(d) that the LSP relic density becomes quite small if m is small, for all experimentally allowed combinations of the remaining parameters. Imposing an upper bound on m therefore leads to an upper bound on Ωh^2; conversely, requiring the neutralino relic density to be larger than some minimal value can give a lower bound on m. We have already seen that for fixed m the annihilation cross section of a b-ino-like LSP becomes small both at very small and at very large m_χ. In the experimentally allowed [48] region $m_\chi \geq 20$ GeV and for $m \leq 140$ GeV, Ωh^2 is maximized if $|M|$ is chosen as large as is allowed by the condition $m_{\tilde{\tau}_1} \geq m_\chi$. Since $m_{\tilde{\tau}_1}$ decreases at large $|\tan\beta|$, Ωh^2 will be maximal at small values of $|\tan\beta|$ where all three SU(2) singlet sleptons are essentially mass degenerate. On the other hand, $m_{\tilde{\tau}_1} = m_\chi$ allows $M^2 \gg m^2$, which means that all other sfermions will be too heavy to contribute significantly to the annihilation cross section, so that Eq. (31) applies. Normalizing the cross section from numerical results of Fig. 1 as before, we find

$$\Omega h^2 \leq 0.47 \left(\frac{m}{100 \text{ GeV}} \right)^2 + 0.085 , \tag{38}$$

where the constant term comes from the D term contribution to $m_{\tilde{l}_R}$, which can be significant for small values of m; we have checked numerically that the true bound deviates from (38) by only 10% or so. For $m > 140$ GeV the maximum of Ωh^2 for fixed m is reached if m_χ is at its experimental lower bound; however, in this region Eq. (38) already allows $\Omega h^2 \geq 1$ anyway.

As discussed above, the bound (38) is saturated if $m_\chi = m_{\tilde{l}_R}$, which implies $m_\chi = 2.42m$ or $M = 5.7m$; all sparticle masses would then be substantially larger than m. We have therefore also studied the question how an upper bound on a physical sparticle mass affects the upper bound on Ωh^2. We find that fixing the mass of the gluino, of the lighter top squark, or of the lightest neutralino or chargino state does not induce a significant upper bound on Ωh^2. On the other hand, we have seen repeatedly that SU(2) singlet sleptons have an important effect on the LSP relic density. Since b-ino-like LSP's annihilate predominantly via $\tilde{l}_R$ exchange, a light $\tilde{l}_R$ implies a small neutralino relic density; this has already been observed by Roszkowski [33].

If χ is a pure b-ino, the annihilation cross section (31) is minimized and Ωh^2 is maximized for given $m_{\tilde{l}_R}$ if m_χ is as small as experimentally allowed [48], $m_\chi = 20$ GeV. For small m_χ and correspondingly small $|M|$ the mass splitting between sfermions need not be large; the contributions from all $f\bar{f}$ final states will then have to be included in Eq. (31), properly weighted with the fourth power of the hypercharge of the exchanged sfermion, and with the sfermion masses given by Eq. (22). The resulting prediction for the maximum of Ωh^2 as a function of $m_{\tilde{l}_R}$ is shown by the dotted curve in Fig. 8. The other curves in this figure are results from numerical scans of the entire allowed parameter space, using the program MINUIT of the CERN program library.

We see that the extended version of Eq. (31) does describe the overall trend of the numerical results; however, the deviation from the full numerical bounds can be as large as a factor of 2 here. In particular, for small values of $m_{\tilde{l}_R}$, Ωh^2 can be substantially *larger* than one would expect for a pure b-ino. This occurs if χ is a light, strongly mixed state. Such a light state exists [43] if $|M|$ and $|\mu|$ are both $O(M_Z)$ and $M_1 \mu \tan\beta > 0$. In this case the SU(2) and $U(1)_Y$ components of χ can have opposite signs (unlike the familiar case of a photino); moreover, the squared b-ino component of this state only amounts to typically 50%. As a result, its couplings to charged sleptons are strongly suppressed [43]. On the other hand, such a state always has sizable Higgsino components and thus couples to gauge and Higgs bosons. For $m_t \geq 130$ GeV and present experimental bounds on sparticle masses the suppression of the slepton masses is the more important effect if $m_{\tilde{l}_R} \leq 150$ GeV; since the existence of such a light mixed LSP also implies [43] a rather light chargino the actual numerical value of the upper bound on Ωh^2 is in this region largely determined by the LEP chargino and neutralino search limits (29a) and (29c). For $m_{\tilde{l}_R} > 150$ GeV the enhancement of the $Z\chi\chi$ and $h\chi\chi$ couplings overcompensates the suppression of the couplings to sleptons; in this case choosing χ to be b-ino-like does indeed maximize Ωh^2, and the full numerical result comes out quite close to the simple approximation based on Eq. (31).

The curve for $m_t = 110$ GeV looks quite different from

those for larger values of m_t. One reason is that for $m_{\tilde{l}_R} \leq 75$ GeV the Higgs search limits now force one to choose $|\tan\beta|$ substantially larger than 1; this increases the $Z\chi\chi$ coupling, which vanishes for $|\tan\beta|=1$. In this region Ωh^2 is therefore again maximized by choosing χ to be b-ino- or photino-like. For larger values of $m_{\tilde{l}_R}$, the constraints imposed by the Higgs search limits are less severe, since the Higgs-boson masses tend to increase with the overall SUSY-breaking scale; for 80 GeV $\leq m_{\tilde{l}_R} \leq 130$ GeV the curve for $m_t=110$ GeV is therefore close to those for a heavier top quark. However, for even larger values of $m_{\tilde{l}_R}$, Ωh^2 is maximized for such small values of $|M/m|$ that radiative gauge symmetry breaking with a light top quark can only be achieved if $|A/m|$ is quite large, which greatly reduces the mass of the lighter top-squark eigenstate; the bound $m_{\tilde{t}_1} \geq 45$ GeV then rules out large regions of parameter space, causing the curve for $m_t=110$ GeV to again fall below those for larger values of m_t if $m_{\tilde{l}_R} > 130$ GeV.

In all cases we find that the upper bound on Ωh^2 for light $\tilde{l}_R$ is determined not only by $m_{\tilde{l}_R}$ itself, but also by the experimental bounds on the masses of the other sparticles and Higgs bosons. This dependence is further illustrated by the long-short dashed curve in Fig. 8, which is valid for $m_t=140$ GeV after we impose the (hypothetical) bounds $m_{\tilde{t}_1,\tilde{\chi}^+} \geq 80$ GeV and $m_{\tilde{g}} \geq 200$ GeV. This is meant to approximate the bounds that would emerge if LEP200 and the Tevatron fail to find evidence for supersymmetry (other than perhaps light sleptons). The constraints from searches for Higgs bosons and neutralinos will also become more severe in the next few years, but the final bounds depend quite strongly on the energy and luminosity that will be achieved in the LEP upgrade.

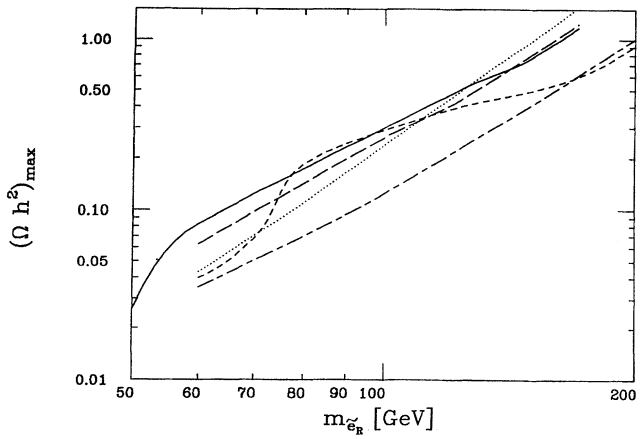

FIG. 8. Upper bounds on Ωh^2 as a function of the mass $m_{\tilde{l}_R}$ of the SU(2)-singlet sleptons. The long dashed, solid, and short dashed curves are for $m_t=110$, 140, and 170 GeV, respectively, and present experimental bounds on sparticle masses; the long-short dashed curve is valid if the lower bounds on the masses of charged sparticles and gluinos are raised to 80 and 200 GeV, respectively, for $m_t=140$ GeV. The dotted curve is based on a simple analytical approximation that assumes that the LSP is a pure b-ino, as described in the text.

The increased bound on the chargino mass excludes a mixed LSP unless [43] $m_\chi \geq 40$ GeV, which is quite close to the Z pole; the upper bound on Ωh^2 is therefore now always saturated if χ is a b-ino- or photino-like state. The increased lower bound on the gluino mass implies $m_\chi > 35$ GeV for such a state [see Eq. (23)]; this enhances the annihilation cross section by approximately a factor of 2, compared to the present bound $m_\chi \geq 20$ GeV. Since χ is now always gauginolike, the bound that can be derived from Eq. (31) reproduces the long-short dashed curve to an accuracy of about 20%.

V. SUMMARY AND CONCLUSIONS

In this paper we have computed the relic density Ωh^2 of LSP's produced during the big bang, within the framework of minimal $N=1$ supergravity models with radiative gauge symmetry breaking. In Sec. II we briefly described the calculation of the relic density for a given LSP annihilation cross section. We then discussed the various contributions to this cross section, including final states composed of gauge and Higgs bosons that become accessible for a "heavy" LSP, $m_\chi > M_W$. Expressions for all these cross sections are given in the Appendix, for a general neutralino eigenstate; to our knowledge such a complete list does not exist in the literature. In Sec. II B we discussed the qualitative features of the most important contributions to the annihilation cross section for the important special cases that the LSP is an almost pure Higgsino or b-ino. In particular, we pointed out that, even though the Higgsino component of a b-ino-like LSP vanishes as $m_\chi \to \infty$, the matrix elements for $\chi\chi \to VV$ and $\chi\chi \to VH$ remain *finite*, where $V=W,Z$ and H is a Higgs boson. This is because of the enhanced production of longitudinal gauge bosons; the same result can also be derived from the equivalence theorem.

In Sec. II C we briefly summarized the constraints imposed on the particle spectrum by the assumption of minimal supergravity (SUGRA). The relations between the masses of the gauginos and those of the superpartners of the light quarks and leptons are by now well known, and have been included in several previous analyses [21–24]. However, SUGRA also implies relations between the mass of the top quark and the soft breaking parameters on the one hand, and the masses of the Higgs bosons as well as the supersymmetric Higgs-boson (Higgsino) mass parameter μ on the other; these relations had previously only been included [25,27] for the case that the SUSY-breaking gaugino mass M is much larger than the scalar mass m at the GUT scale. We saw in our numerical examples of Sec. III that these relations can have large effects on the relic density. In particular, we found that the coupling of a b-ino-like LSP to gauge and Higgs bosons is usually suppressed for a heavy top quark and/or large m, since increasing m_t or m tends to increase $|\mu|$, which in turn reduces the Higgsino component of χ. This strongly affects Ωh^2 both in the pole region ($m_\chi \simeq M_Z/2$) and in the threshold region ($m_\chi \simeq M_Z$). Moreover, as already pointed out in Ref. [32], Ωh^2 is greatly reduced if the ratio $\tan\beta$ of the VEV's of the two Higgs bosons is large, since this implies large b and τ Yukawa couplings, and thus a light pseudoscalar Higgs boson P and reduced masses for the light

$\tilde{b}$ and $\tilde{\tau}$ eigenstates.

The relations between particle masses and neutralino couplings imposed by SUGRA also imply that the region of parameter space where the LSP density can lead to a flat universe ($0.25 \leq \Omega h^2 \leq 1$), as predicted by inflationary models, has a very complicated shape, since the $\chi\chi$ annihilation cross section depends on *all* input parameters; the same is true for the region where LSP's can at least provide the DM halo of galaxies ($\Omega h^2 \geq 0.025$). Nevertheless it is clear from the results of Sec. III that a cosmologically interesting relic density is obtained quite naturally, provided that χ is gauginolike and the SUSY-breaking parameter m is not too small. If χ is Higgsino-like and $m_\chi > M_W$, $\chi\chi$ annihilation into pairs of gauge bosons is so strong that cosmologically interesting values of Ωh^2 only occur [18,19] for $m_\chi > 0.5$ TeV. Since in minimal SUGRA the gluino as well as most squarks are at least 6 times heavier than the LSP, requiring $m_\chi > 0.5$ TeV leads to quite severe fine-tuning [35,16] and is thus unattractive. The $\chi\chi$ annihilation cross section for Higgsino-like χ can be quite small below the WW threshold if the gaugino mass $|M|$ is large; however, using results of Ref. [37] we estimated that in this case coannihilation of χ with the next-to-lightest neutralino χ' will suppress Ωh^2 to a value well below 0.25, since the off-diagonal $Z\chi\chi'$ coupling is large, and since coannihilation can proceed from an s-wave initial state. We therefore conclude that the Higgsino does not make a very attractive DM candidate in minimal SUGRA models.

Unfortunately, we saw in Sec. IV that the complicated shape of the region of parameter space that yields $\Omega h^2 \leq 1$ makes it difficult to derive interesting upper bounds on mass parameters from the requirement that relic neutralinos do not overclose the Universe. In particular, m can be almost arbitrarily large, and thus all sfermions and most Higgs bosons can be very heavy, if $m_\chi \simeq M_Z/2$ or $m_\chi \simeq m_h/2$, where h denotes the light scalar Higgs boson. In this case the gluino, the lighter chargino and the next-to-lightest neutralino would still lie in the region accessible to the next generation of accelerators ($m_{\tilde{g}} \leq 500$ GeV, $m_{\tilde{\chi}^+,\chi'} \leq 150$ GeV). However, if $|\tan\beta|$ is large, m_P can be greatly reduced so that m_χ can be close to $m_P/2$. Since P exchange mediates $\chi\chi$ annihilation from an s-wave state, Ωh^2 is greatly suppressed in this case, allowing both m and $|M|$ to be well beyond 1 TeV without getting in conflict with cosmology. If the top quark is not very heavy, $m_t \leq 155$ GeV, cosmologically safe solutions with very large m and $|M|$ also exist for small $|\mu|$, so that the LSP is Higgsino-like. In this case one would still have a "light," almost degenerate SU(2) doublet of Higgsinos, but all other sparticles would be very heavy. Since the mass splitting could be as small as ~ 1 GeV, such light Higgsinos would probably be very difficult to observe even at e^+e^- colliders [60]. This scenario is therefore very similar to the case of a very large m_χ as far as collider experiments are concerned. We have to conclude that the requirement $\Omega h^2 \leq 1$ does not strictly exclude the possibility that sparticle masses are well beyond the reach even of the planned supercolliders.

On the other hand, interesting upper bounds can be obtained for the "generic" case of a b-ino-like LSP away from poles. We found that in this case the total annihilation cross section is dominated by the l^+l^- final state produced via $\tilde{l}_R$ exchange ($l = e,\mu,\tau$). Contributions from $\tilde{l}_L$ exchange and $\tilde{q}$ exchange are suppressed by the larger masses and smaller hypercharges of these sfermions, while the contribution from Z exchange is suppressed by the small $Z\chi\chi$ coupling. We mentioned earlier that the VV and Zh final states also contribute with full gauge strength if the LSP is sufficiently heavy, but the relevant hypercharge here is the one of the Higgs bosons, leading to a suppression factor of $\frac{1}{16}$ compared to the $\tilde{l}_R$ exchange contribution. This allowed us to derive the very simple and yet quite accurate expression (31) for the total annihilation cross section, leading to the analytically derived bounds (35) and (36). In particular, we find for this case an upper bound $m_{\tilde{g}} \leq 2$ TeV, which is only slightly less stringent than the bound derived [16,35] from the requirement that fine-tuning should occur at most at the 10% level; the corresponding bound on m_χ is considerably more stringent than the one that follows under similar assumptions [18] in a more general SUSY model. Our bound $m \leq 300$ GeV is potentially even more interesting, since this value is *below* the one derived [16,35] from fine-tuning arguments; together with the bound on $m_{\tilde{g}}$ it would virtually guarantee that at least the sleptons, the light chargino and the next-to-lightest neutralino should be observed at a TeV e^+e^- supercollider. However, we have to remind the reader that there are several ways to evade these bounds.

As first pointed out in Ref. [22] and also emphasized in Refs. [23,24], the LSP relic density can only lead to a flat universe with $0.5 \leq h \leq 1$ if m is not too small. We quantified this in the simple relation (38), which shows that $\Omega h^2 \geq 0.25$ is only possible for $m \geq 40$ GeV. (In Ref. [24] the more stringent bound $m \geq 100$ GeV has been found, but this is only valid for $m_\chi \leq M_W$.) Furthermore, requiring $\Omega h^2 \geq 0.25$ also implies a lower bound on the mass of SU(2) singlet sleptons. The exact value of this bound depends on the top mass, as well as on the bounds on the masses of other sparticles and Higgs bosons, but it is always close to 100 GeV (see Fig. 8). We thus see that requiring $0.25 \leq \Omega h^2 \leq 1$ determines $m_{\tilde{l}_R}$ to be within a factor of 2 of 200 GeV, *if* the LSP is gauginolike and not near a pole. Unfortunately, in this case LEP200 will fail to discover a slepton. This has already been pointed out in Ref. [33] for a light LSP, but at least within the framework of SUGRA models this conclusion also holds $m_\chi \geq M_W$. (Of course, we need $m_\chi \leq m_{\tilde{l}_R}$ always.) On the other hand, the gaugino mass parameter M is only poorly determined by the requirement that Ωh^2 lies in the cosmologically interesting range, since the annihilation cross section is almost independent of M over a wide range (see Figs. 1). In particular, the gluino, the squarks, the lighter chargino and at least one neutralino could all lurk "just around the corner," but their masses could also lie in the range that can only be covered by supercolliders.

Our overall conclusion is that, while limits on the relic

neutralino density allow to rule out large regions of parameter space, they do not allow to derive upper bounds on sparticle masses which are both interesting for experiments at existing or planned colliders and valid for all combinations of the other parameters. On the other hand, results for the perhaps most natural case of a gauginolike LSP do indicate that sparticle masses should lie in the range to be covered by planned e^+e^- and pp supercolliders. Moreover, if the dark matter in our Galaxy does indeed consist of neutralinos, one would expect their mass to lie within the range of sensitivity [61] of next-generation direct search experiments and [62] of experiments looking for neutralino annihilation in the Sun, although a strict lower bound on the expected signal size is again difficult to derive. Cosmological arguments can therefore supplement and lend support to direct SUSY searches at collider experiments.

Note added in proof. After submission of our paper, a more detailed investigation of the effects of coannihilation on the relic density of Higgsino-like LSP's was performed by S. Mizuta and M. Yamaguchi, Tohoku Univeristy Report No. TU-409, 1992 (unpublished). They confirm our rough estimate (33) for the influence of coannihilation of the LSP with the next-to-lightest neutralino. However, they also point out that for most combinations of parameters, the next-to-lightest sparticle is actually a Higgsino-like chargino. This suppresses the relic density even further. As a result, a Higgsino-like LSP cannot even provide the DM halo of galaxies, unless its mass exceeds several hundred GeV.

ACKNOWLEDGMENTS

We thank K. Hikasa for sharing his expertise in the calculation of helicity amplitudes with us, as well as for many useful discussions. M.M.N. thanks the theory group at KEK, and M.D. the theory group at SLAC and the Institute of Particle Physics Phenomenology in Madison, Wisconsin, for their kind hospitality. The work of M.M.N. was supported in part by a Grant-in-Aid for scientific research from the Ministry of Education, Science,and Culture, No. 02952050.

APPENDIX A: MATRIX ELEMENTS

Since we are interested in the nonrelativistic limit of the $\chi\chi$ annihilation cross section, we employ the partial wave formalism. In this formalism the helicity amplitude for the process

$$\chi(h)+\chi(\bar{h})\rightarrow X(\lambda_X)+Y(\lambda_Y) \tag{A1}$$

(h, $\bar{h}$, λ_X, and λ_Y are the helicities of the corresponding particles) is expanded as follows:

$$T=\sum_{L=0}^{\infty}\sum_{S=0}^{1}\sum_{J=|L-S|}^{L+S} A(^{2S+1}L_J)\mathcal{P}(^{2S+1}L_J)d^J_{\lambda_i,\lambda_f} . \tag{A2}$$

Here the reduced partial wave amplitude A describes annihilation from an initial state with definite spin S and orbital angular momentum L, and thus also with definite C and P quantum numbers. The spin projectors $\mathcal{P}$ depend only on h and $\bar{h}$, and the angular dependence is contained in the d functions $d^J_{\lambda_i,\lambda_f}$. $\lambda_i=h-\bar{h}$ and $\lambda_f=\lambda_X-\lambda_Y$ are the differences of the helicities of the initial and final particles, respectively. Because our initial state consists of two identical Majorana fermions, we only need to consider initial states with $C=1$. Furthermore, since we want to expand the total annihilation cross section only up to $O(v^2)$, only annihilation from s- and p-wave initial states has to be included. Altogether we thus find that we need to include only the contributions from the $^1S_0$, $^3P_0$, $^3P_1$, and $^3P_2$ initial states; explicit expressions for the relevant $\mathcal{P}$ can be found in Ref. [63]. The annihilation cross section is then given by

$$\sigma(\chi\chi\rightarrow XY)v=\frac{1}{4}\frac{\bar{\beta}_f}{8\pi sS}\left[|A(^1S_0)|^2+\frac{1}{3}[|A(^3P_0)|^2+|A(^3P_1)|^2+|A(^3P_2)|^2]\right] . \tag{A3}$$

Here v is the relative velocity of initial neutralinos and s is the square of the total energy. S is a symmetry factor which is 2 when $X=Y$. The summation over the final helicities is implicit in this equation. Finally, the kinematical factor $\bar{\beta}_f$ is given by

$$\bar{\beta}_f=\sqrt{1-2(m_X^2+m_Y^2)/s+(m_X^2-m_Y^2)^2/s^2} . \tag{A4}$$

In this Appendix we list the helicity amplitudes $A(^{2S+1}L_J)$ for all two-body final states accessible to $\chi\chi$ annihilation in leading order in perturbation theory. We first list some couplings which appear in many matrix elements:

$$O^L_{0j}=-(1/\sqrt{2})N_{04}V_{j2}+N_{02}V_{j1} , \tag{A5a}$$

$$O^R_{0j}=(1/\sqrt{2})N_{03}U_{j2}+N_{02}U_{j1} , \tag{A5b}$$

$$Q'^L_{0j}=N_{04}V_{j1}+(1/\sqrt{2})(N_{02}+N_{01}\tan\theta_W)V_{j2} , \tag{A5c}$$

$$Q'^R_{0j}=N_{03}U_{j1}-(1/\sqrt{2})(N_{02}+N_{01}\tan\theta_W)U_{j2} , \tag{A5d}$$

$$O''^L_{0j}=-\tfrac{1}{2}N_{03}N_{j3}+\tfrac{1}{2}N_{04}N_{j4} , \tag{A5e}$$

$$Q''_{0j}=\tfrac{1}{2}[N_{03}(N_{j2}-\tan\theta_W N_{j1})+(0\leftrightarrow j)] , \tag{A5f}$$

$$S''_{0j}=\tfrac{1}{2}[N_{04}(N_{j2}-\tan\theta_W N_{j1})+(0\leftrightarrow j)] . \tag{A5g}$$

The expressions for O^L, O^R, Q'', S'', and O''^L are the same as in Ref. [6]; our definitions for Q'^L, and Q'^R, differ slightly from those of Ref. [42]. U and V are the matrices that diagonalize the chargino mass matrix $\mathcal{M}^{\pm}$, which is given by [6]

$$\mathcal{M}^{\pm}=\begin{pmatrix} M_2 & M_W\sqrt{2}\sin\beta \\ M_W\sqrt{2}\cos\beta & \mu \end{pmatrix} . \tag{A6}$$

The matrices U and V can be chosen to be real:

$$U=\begin{pmatrix} \cos\phi_- & \sin\phi_- \\ -\sin\phi_- & \cos\phi_- \end{pmatrix} ,$$
$$V=\begin{pmatrix} \cos\phi_+ & \sin\phi_+ \\ -\sin\phi_+ & \cos\phi_+ \end{pmatrix} . \tag{A7}$$

In the limit where either $|M_2|$ or $|\mu|$ is much larger than M_W, the chargino mass eigenstates are almost identical to

the current states. The (small) mixing angles then become

$$\phi_- = \frac{\sqrt{2}M_W}{M_2^2-\mu^2}(M_2\cos\beta+\mu\sin\beta)\ , \tag{A8a}$$

$$\phi_+ = \frac{\sqrt{2}M_W}{M_2^2-\mu^2}(M_2\sin\beta+\mu\cos\beta)\ . \tag{A8b}$$

The N_{ij} in Eqs. (A5) are elements of the matrix that diagonalize the neutralino mass matrix, Eq. (4); as already discussed in Sec. II B, it also becomes almost diagonal if $|M_2|$ or $|\mu|$ is very large [see Eqs. (6)]. Unlike Refs. [6] and [42], we do not require the chargino and neutralino masses to be positive; N_{ij} can therefore also be chosen to be real. We have checked by explicit calculation that this still preserves all relative signs in our amplitudes, provided we keep the sign of the fermion masses everywhere. Finally, the suffix zero in Eqs. (A5) refers to the lightest neutralino χ.

The coupling of the neutral Higgs bosons to neutralinos can be expressed in terms of Q'' and S'' [42]:

$$T_{P0j} = -\sin\beta Q''_{0j}+\cos\beta S''_{0j}\ , \tag{A9a}$$

$$T_{10j} = -\cos\alpha Q''_{0j}+\sin\alpha S''_{0j}\ , \tag{A9b}$$

$$T_{20j} = \sin\alpha Q''_{0j}+\cos\alpha S''_{0j}\ . \tag{A9c}$$

Here the labels P, 1, and 2 refer to the pseudoscalar and the heavier and lighter neutral scalar; α in Eqs. (A9) is the mixing angle of the neutral scalar Higgs bosons as defined in Ref. [42], including leading one-loop radiative corrections.

Finally, we define some kinematical quantities and propagators:

$$\Delta^2 = \frac{(m_X^2+m_Y^2)}{2m_\chi^2}\ ; \tag{A10a}$$

$$P_I = 1+R_I^2-(R_X^2+R_Y^2)/2\ ; \tag{A10b}$$

$$R_X = m_X/m_\chi,\quad R_Y = m_Y/m_\chi,\quad R_I = m_I/m_\chi\ . \tag{A10c}$$

Here, m_I is the mass of an exchanged particle, and P_I is the $v\to 0$ limit of the inverse of the corresponding t- or u-channel propagator.

We are now ready to list the partial wave amplitudes of the contributing processes. As mentioned above, we only need the nonrelativistic limit of the annihilation cross section, i.e., its expansion in powers of v up to and including terms of $O(v^2)$. However, this expansion breaks down [37] in the vicinity of poles and thresholds, since there the "higher order" terms can actually diverge. In our expressions below we therefore only include those terms of order v^2 that result from the expansion of *well-behaved* functions of v. Specifically, we include terms that result from the expansion of t- and u-channel propagators, as well as terms that result from the calculation of spinors or bosonic wave functions. On the other hand, we do *not* expand the kinematical function $\bar\beta_f$, nor s-channel propagators. Of course, far away from the threshold or pole, these terms can be expanded safely. This can be incorporated into our matrix elements by the following substitutions:[15]

$$\bar\beta_f \to \bar\beta_f(v=0)+\frac{v^2}{8\bar\beta_f(v=0)}\left[\Delta^2-\frac{(m_X^2-m_Y^2)^2}{8m_\chi^4}\right]\ ; \tag{A11a}$$

$$\frac{1}{4-R_I^2}\to\frac{1}{4-R_I^2}\left[1-\frac{v^2}{4-R_I^2}\right]\ . \tag{A11b}$$

Clearly, these substitutions should only be used in the $O(v^0)$ terms of the $^1S_0$ amplitudes. Because of the suppression factor $3/x_F$ in the expression (3) for Ωh^2, as well as the smallness of the numerical factors in Eq. (A11a), the numerical effect of these substitutions is only sizable in cases where the expansion itself can no longer be trusted; in this case only the much more complicated methods described in Ref. [37] give reliable results. Since a more careful treatment of poles and thresholds will not change our conclusions, we do not pursue this avenue here. It should be noted that the $O(v)$ terms that result from the expansion of t- and u-channel propagators can, e.g., change the annihilation cross section into $f\bar f$ final states by a factor of two; fortunately the $O(v)$ terms are always regular.

We list contributions with different final state helicities separately; all these contributions have to be added incoherently, as shown in Eq. (A3).

1. $\chi\chi\to W^-(\lambda)W^+(\bar\lambda)$

This final state receives contributions from the exchange of the two chargino eigenstates (labeled by j) in the t or u channel, as well as from the exchange of the two neutral scalar Higgs bosons (labeled by i) as well as the Z boson in the s channel. In the following expressions, summation over subscripts $(i,j,\ldots)$ that appear more than once is always understood:

$A(^1S_0)$: $\lambda_f=0$, $\lambda=\pm1$,

$$2\sqrt{2}\bar\beta_f g^2\frac{O_{0j}^{L\,2}+O_{0j}^{R\,2}}{P_j}+\sqrt{2}v^2\bar\beta_f g^2\left[\frac{2}{3}\frac{R_j^+}{P_j^2}O_{0j}^L O_{0j}^R+\frac{O_{0j}^{L\,2}+O_{0j}^{R\,2}}{P_j}\left[\frac{1}{4}-\frac{4}{3P_j}+\frac{2\bar\beta_f^2}{3P_j^2}\right]\right]\ ; \tag{A12a}$$

$A(^3P_0)$: $\lambda_f=0$, $\lambda=0$,

$$\frac{\sqrt{6}vg^2}{R_W^2}\left[-\frac{4}{3}\frac{O_{0j}^{L\,2}+O_{0j}^{R\,2}}{P_j}+\frac{4O_{0j}^L O_{0j}^R R_j^+}{P_j}\left[1-\frac{2}{3P_j}\right]\right]$$

[15] Far away from the pole, the propagator can be taken to be real.

$$+\sqrt{6}vg^2\left[\frac{O_{0j}^{L\,2}+O_{0j}^{R\,2}}{P_j}\left[1-\frac{2\bar{\beta}_f^2}{3P_j}\right]-\frac{2O_{0j}^L O_{0j}^R R_j^+}{P_j}\left[1-\frac{4}{3P_j}\right]\right]-\frac{\sqrt{6}v(1+\bar{\beta}_f^2)g^2F_i}{(4-R_{H_i}^2+iG_{H_i})R_W}\ ; \tag{A12b}$$

$\lambda_f=0,\ \lambda=\pm1$,

$$\sqrt{6}vg^2\left[\frac{O_{0j}^{L\,2}+O_{0j}^{R\,2}}{P_j}\left[\frac{1}{3}-\frac{2\bar{\beta}_f^2}{3P_j}\right]-\frac{2O_{0j}^L O_{0j}^R R_j^+}{P_j}\right]+\frac{\sqrt{6}vg^2R_WF_i}{4-R_{H_i}^2+iG_{H_i}}\ ; \tag{A12c}$$

$A(^3P_1)$: $|\lambda_f|=1$,

$$\frac{2v\bar{\beta}_f^2\lambda_f g^2}{R_W}\left[\frac{O_{0j}^{L\,2}+O_{0j}^{R\,2}}{P_j}\left[1-\frac{1}{P_j}\right]-\frac{2O_{0j}^L O_{0j}^R R_j^+}{P_j^2}\right]+2v\bar{\beta}_f g^2\frac{O_{0j}^{L\,2}-O_{0j}^{R\,2}}{R_WP_j}\left[2-\frac{\bar{\beta}_f^2}{P_j}\right]-\frac{8v\bar{\beta}_f g^2O_{00}''^L}{R_W(4-R_Z^2)}\ ; \tag{A12d}$$

$\lambda_f=0,\ \lambda=0$,

$$\frac{2v\bar{\beta}_f}{R_W^2P_j}(3-\bar{\beta}_f^2)g^2(O_{0j}^{L\,2}-O_{0j}^{R\,2})-\frac{4v\bar{\beta}_f g^2O_{00}''^L}{(4-R_Z^2)R_W^2}(3-\bar{\beta}_f^2)\ ; \tag{A12e}$$

$\lambda_f=0,\ \lambda=\pm1$,

$$\frac{2v\bar{\beta}_f}{P_j}g^2(O_{0j}^{L\,2}-O_{0j}^{R\,2})-\frac{4v\bar{\beta}_f g^2O_{00}''^L}{4-R_Z^2}\ ; \tag{A12f}$$

$A(^3P_2)$: $|\lambda_f|=2$,

$$-\frac{2\sqrt{2}v}{P_j}g^2(O_{0j}^{L\,2}+O_{0j}^{R\,2})\ ; \tag{A12g}$$

$|\lambda_f|=1$,

$$\frac{2vg^2}{R_W}\left[\frac{-R_j^{+\,2}}{P_j^2}(O_{0j}^{L\,2}+O_{0j}^{R\,2})+\frac{2O_{0j}^L O_{0j}^R R_j^+}{P_j^2}\bar{\beta}_f^2+\lambda_f\bar{\beta}_f^3\frac{O_{0j}^{L\,2}-O_{0j}^{R\,2}}{P_j^2}\right]\ ; \tag{A12h}$$

$\lambda_f=0,\ \lambda=\pm1$,

$$\frac{2vg^2}{\sqrt{3}}(O_{0j}^{L\,2}+O_{0j}^{R\,2})\frac{1-R_j^{+\,2}-R_W^2}{P_j^2}\ ; \tag{A12i}$$

$|\lambda_f|=0,\ \lambda=0$,

$$\frac{4vg^2}{\sqrt{3}R_W^2}\left[-\frac{O_{0j}^{L\,2}+O_{0j}^{R\,2}}{P_j}\left[1-\bar{\beta}_f^2\frac{R_W^2}{P_j}\right]+4\bar{\beta}_f^2\frac{O_{0j}^L O_{0j}^R R_j^+}{P_j^2}\right]\ . \tag{A12j}$$

Here, the R are the rescaled masses of exchanged or final state particles [see Eq. (A10c)], and we have introduced the rescaled widths

$$G_{H_i}=\Gamma_{H_i}m_{H_i}/m_\chi^2\ . \tag{A13}$$

The definition of the P_j is as in Eq. (A10b), and the F_i are given by [42]

$$F_1=\cos(\beta-\alpha)T_{100},\quad F_2=\sin(\beta-\alpha)T_{200}\ . \tag{A14}$$

2. $\chi\chi\to Z(\lambda)Z(\bar{\lambda})$

Here the contributing diagrams are very similar to those of the W^+W^- final state, except that the Z exchange contribution is absent. Moreover, the subscript j now labels the four neutralino eigenstates. The nonvanishing partial wave amplitudes can be written as

$A(^1S_0)$: $\lambda_f=0,\ \lambda=\pm1$,

$$\frac{4\sqrt{2}\bar{\beta}_f g_Z^2O_{0j}''^{L\,2}}{P_j}+2\sqrt{2}v^2\bar{\beta}_f g_Z^2O_{0j}''^{L\,2}\left[-\frac{R_j}{3P_j^2}+\frac{1}{P_j}\left[\frac{1}{4}-\frac{4}{3P_j}+\frac{2\bar{\beta}_f^2}{3P_j^2}\right]\right]\ ; \tag{A15a}$$

$A(^3P_0)$: $\lambda_f=0$, $\lambda=0$,

$$\frac{4\sqrt{6}vg_Z^2}{R_Z^2}O_{0j}''^{L^2}\left[-\frac{2}{3P_j}-\frac{R_j}{P_j}\left[1-\frac{2}{3P_j}\right]\right]$$

$$+2\sqrt{6}vg_Z^2O_{0j}''^{L^2}\left[\frac{1}{P_j}\left[1-\frac{2\bar{\beta}_f^2}{3P_j}\right]+\frac{R_j}{P_j}\left[1-\frac{4}{3P_j}\right]\right]-\frac{\sqrt{6}vg^2(1+\bar{\beta}_f^2)F_i}{(4-R_{H_i}^2+iG_{H_i})R_W}\ ; \quad \text{(A15b)}$$

$\lambda_f=0$, $\lambda=\pm1$,

$$2\sqrt{6}vg_Z^2O_{0j}''^{L^2}\left[\frac{1}{P_j}\left[\frac{1}{3}-\frac{2\bar{\beta}_f^2}{3P_j}\right]+\frac{R_j}{P_j}\right]+\frac{\sqrt{6}vg_Z^2R_WF_i}{4-R_{H_i}^2+iG_{H_i}}\ ; \quad \text{(A15c)}$$

$A(^3P_1)$: $|\lambda_f|=1$,

$$\frac{4v\bar{\beta}_f^2\lambda_fg_Z^2O_{0j}''^{L^2}}{R_Z}\left[\frac{1}{P_j}\left[1-\frac{1}{P_j}\right]+\frac{R_j}{P_j^2}\right]\ ; \quad \text{(A15d)}$$

$A(^3P_2)$: $|\lambda_f|=2$

$$-(4\sqrt{2}vg_Z^2/P_j)O_{0j}''^{L^2}\ ; \quad \text{(A15e)}$$

$|\lambda_f|=1$,

$$-\frac{4vg_Z^2}{R_Z}O_{0j}''^{L^2}\left[\frac{R_j^2}{P_j^2}+\frac{R_j}{P_j^2}\bar{\beta}_f^2\right]\ ; \quad \text{(A15f)}$$

$|\lambda_f|=0$, $\lambda=\pm1$,

$$\frac{4vg_Z^2}{\sqrt{3}}O_{0j}''^{L^2}\frac{1-R_j^2-R_Z^2}{P_j^2}\ ; \quad \text{(A15g)}$$

$|\lambda_f|=0$, $\lambda=0$,

$$-\frac{8vg_Z^2}{\sqrt{3}R_Z^2}O_{0j}''^{L^2}\left[\frac{1}{P_j}\left[1-\frac{R_Z^2\bar{\beta}_f^2}{P_j}\right]+\frac{2R_j\bar{\beta}_f^2}{P_j^2}\right]\ . \quad \text{(A15h)}$$

In Eqs. (A15) we have used the usual notation

$$g_Z=g/\cos\theta_W\ . \quad \text{(A16)}$$

3. $\chi\chi\to Z(\lambda)H_a$

This final state receives contributions from the exchange of the four neutralinos (labeled by j) in the t or u channel, as well as from the s-channel exchange of the Z boson as well as of the pseudoscalar Higgs boson P. The result is

$A(^1S_0)$: $\lambda=0$,

$$-\frac{2\sqrt{2}\bar{\beta}_f}{R_Z}gg_Z\left[\frac{2J_j(R_j-1)}{P_j}+\frac{O}{R_Z\cos\theta_W}-\frac{4L}{4-R_P^2+iG_P}\right]$$

$$-v^2\frac{\sqrt{2}\bar{\beta}_f}{R_Z}gg_Z\frac{J_j}{P_j}\left[\frac{1}{2}(R_j-5)-\frac{2(R_j-1)}{P_j}+\frac{4(R_j-1)}{3P_j^2}\bar{\beta}_f^2+(2-\Delta^2)\frac{2}{3P_j}\right]$$

$$+v^2\frac{\sqrt{2}\bar{\beta}_f}{R_Z}gg_Z\left[\frac{3L}{4-R_P^2+iG_P}-\frac{O}{4R_Z\cos\theta_W}\right]\ ; \quad \text{(A17a)}$$

$A(^3P_1)$: $\lambda=\pm1$,

$$-4vgg_Z\frac{J_j}{P_j^2}\left[R_j^2-\frac{\delta^4}{4}\right]-4vgg_Z\frac{J_jR_j}{P_j}+2vg_Z^2O\frac{R_Z}{4-R_Z^2}\ ; \quad \text{(A17b)}$$

$\lambda=0$,

$$-2\frac{v}{R_Z}\left[1+\frac{\delta^2}{2}\right]gg_Z\left[2(1+R_j)\frac{J_j}{P_j}-\frac{R_Z}{\cos\theta_W(4-R_Z^2)}O\right]; \tag{A17c}$$

$A(^3P_2)$: $\lambda=\pm1$,

$$-4\lambda v\bar{\beta}_f^2 gg_Z(J_j/P_j^2) . \tag{A17d}$$

In addition to Δ, which has already been defined in Eq. (A10a), we have introduced the quantities

$$G_P=\Gamma_P m_P/m_\chi^2 , \tag{A18a}$$

$$\delta^2=(R_Z^2-R_{H_a}^2)/2 , \tag{A18b}$$

$$J_j=-O_{0j}''^L T_{a0j} \quad \text{for } H_a , \tag{A18c}$$

$$L=\tfrac{1}{2}\sin(\alpha-\beta)T_{P0j} \quad \text{for } H_1 , \tag{A18d}$$

$$=\tfrac{1}{2}\cos(\alpha-\beta)T_{P0j} \quad \text{for } H_2 , \tag{A18e}$$

$$O=O_{0j}''^L\cos(\alpha-\beta) \quad \text{for } H_1 , \tag{A18f}$$

$$=O_{0j}''^L\sin(\beta-\alpha) \quad \text{for } H_2 . \tag{A18g}$$

4. $\chi\chi\to Z(\lambda)P$

The contributing diagrams are very similar to those of the ZH final state, except that the single P exchange diagram has to be replaced by H_1, H_2 exchange diagrams; notice that these scalar Higgs bosons cannot be on shell, so that we need not introduce complex propagators here:

$A(^3P_0)$: $\lambda=0$,

$$4\sqrt{6}\frac{v\bar{\beta}_f}{R_Z}gg_Z\left[\left[1+\frac{\delta^2}{2}\right]\frac{K_jR_j}{3P_j^2}-\left[\frac{2}{3}+R_j^2-\frac{2\Delta^2}{3}+\frac{\delta^2}{6}\right]\frac{K_j}{P_j^2}+\frac{L_i}{4-R_{H_i}^2}\right]; \tag{A19a}$$

$A(^3P_1)$: $\lambda=\pm1$,

$$-4v\bar{\beta}_f\lambda_f gg_Z\left[-R_j+\frac{\delta^2}{2}\right]\frac{K_j}{P_j^2}; \tag{A19b}$$

$A(^3P_2)$: $\lambda=\pm1$,

$$4v\bar{\beta}_f gg_Z\left[-R_j+\frac{\delta^2}{2}\right]\frac{K_j}{P_j^2}; \tag{A19c}$$

$\lambda=0$,

$$-\frac{8}{\sqrt{3}}v\bar{\beta}_f gg_Z\frac{K_j}{R_ZP_j^2}\left[1+R_j-\Delta^2+\frac{\delta^2}{2}(R_j-1)\right] . \tag{A19d}$$

In Eqs. (A19) we have defined

$$\delta^2=\tfrac{1}{2}(R_Z^2-R_P^2) , \tag{A20a}$$

$$L_1=\tfrac{1}{2}\sin(\alpha-\beta)T_{100},\quad L_2=\tfrac{1}{2}\cos(\alpha-\beta)T_{200} , \tag{A20b}$$

$$K_j=O_{0j}''^L T_{P0j} . \tag{A20c}$$

5. $\chi\chi\to W^-(\lambda)H^+$

In this case one has contributions from the exchange of the two charginos, which are again labeled by the suffix j, as well as from the exchange of all three neutral Higgs bosons. Notice also that there are equal contributions from W^+H^- and W^-H^+ production, leading to an overall factor of 2 in the final cross section in this case. The contributing partial wave amplitudes are

$A(^1S_0)$: $\lambda=0$,

$$4\sqrt{2}\bar{\beta}_f g^2\frac{J_j'+J_j''}{R_WP_j}+\sqrt{2}v^2\frac{\bar{\beta}_f g^2(J_j'+J_j'')}{R_WP_j}\left[\frac{5}{2}-\frac{2}{P_j}+\frac{4\bar{\beta}_f^2}{3P_j^2}-\frac{2}{3P_j}(2-\Delta^2)\right]$$
$$-4\sqrt{2}\bar{\beta}_f g^2(J_j'-J_j'')\frac{R_j^+}{R_WP_j}-\sqrt{2}\bar{\beta}_f v^2g^2(J_j'-J_j'')\frac{R_j^+}{R_WP_j}\left[\frac{4\bar{\beta}_f^2}{3P_j^2}-\frac{2}{P_j}+\frac{1}{2}\right]$$
$$-4\sqrt{2}\bar{\beta}_f g^2T_{P00}\frac{1}{R_W}\frac{1}{4-R_P^2}\left[1+\frac{3v^2}{8}\right]; \tag{A21a}$$

$A(^3P_0)$: $\lambda=0$,

$$4\sqrt{6}\frac{v\bar{\beta}_f}{R_W}g^2\left[R_j^+\left[1+\frac{\delta^2}{2}\right]\frac{K_j'-K_j''}{3P_j^2}-\left[\frac{2}{3}+R_j^{+2}-\frac{2}{3}\Delta^2+\frac{\delta^2}{6}\right]\frac{K_j'+K_j''}{P_j^2}\right]-\frac{4\sqrt{6}}{R_W}v\bar{\beta}_f\frac{g^2L_i}{4-R_{H_i}^2}; \tag{A21b}$$

$A(^3P_1)$: $\lambda=\pm1$,

$$-4v\left[R_j^{+2}-\frac{\delta^4}{4}\right]g^2\frac{J_j'+J_j''}{P_j^2}-4vg^2(J_j'-J_j'')\frac{R_j^+}{P_j}+\frac{4v\bar\beta_f\lambda}{P_j^2}g^2\left[R_j^+(K_j'-K_j'')-\frac{\delta^2}{2}(K_j'+K_j'')\right]; \tag{A21c}$$

$\lambda=0$,

$$-\frac{4vg^2}{R_W P_j}[(J_j'+J_j'')+(J_j'-J_j'')R_j^+]\left[1+\frac{\delta^2}{2}\right]; \tag{A21d}$$

$A(^3P_2)$: $\lambda=\pm1$,

$$-4v\lambda g^2\frac{J_j'+J_j''}{P_j^2}\bar\beta_f^2+\frac{4v\bar\beta_f}{P_j^2}g^2\left[(K_j'+K_j'')\frac{\delta^2}{2}-R_j^+(K_j'-K_j'')\right]; \tag{A21e}$$

$\lambda=0$,

$$\frac{8v\bar\beta_f g^2}{\sqrt3 R_W P_j^2}\left[\left[-1+\Delta^2+\frac{\delta^2}{2}\right](K_j'+K_j'')-R_j^+\left[1+\frac{\delta^2}{2}\right](K_j'-K_j'')\right]. \tag{A21f}$$

In Eqs. (A21) we have introduced

$$\delta^2=\tfrac12(R_W^2-R_{H^+}^2)\ , \tag{A22a}$$

$$J_j'=-\tfrac14(O_{0j}^R-O_{0j}^L)(Q_{0j}'^R\sin\beta+Q_{0j}'^L\cos\beta)\ , \tag{A22b}$$

$$J_j''=-\tfrac14(O_{0j}^R+O_{0j}^L)(Q_{0j}'^R\sin\beta-Q_{0j}'^L\cos\beta)\ , \tag{A22c}$$

$$K_j'=-\tfrac14(O_{0j}^R-O_{0j}^L)(Q_{0j}'^R\sin\beta-Q_{0j}'^L\cos\beta)\ , \tag{A22d}$$

$$K_j''=-\tfrac14(O_{0j}^R+O_{0j}^L)(Q_{0j}'^R\sin\beta+Q_{0j}'^L\cos\beta)\ . \tag{A22e}$$

6. $\chi\chi\to H_aH_b$ or PP

Both the H_aH_b $(a,b=1,2)$ and the PP final state can be produced by the exchange of one of the four neutralinos (labeled by j) in the t or u channel, as well as by scalar Higgs exchange in the s channel. The contributing amplitudes for the H_aH_b final state can be written as

$$A(^3P_0):\ \sqrt6 vg^2\left[g_{abi}T_{i00}\frac{R_Z}{4-R_{H_i}^2+iG_{H_i}}-2T_{a0j}T_{b0j}\frac{1+R_j}{P_j}+\frac43T_{a0j}T_{b0j}\frac{\bar\beta_f^2}{P_j^2}\right]; \tag{A23a}$$

$$A(^3P_2):\ -(8/\sqrt3)v\bar\beta_f^2g^2T_{a0j}T_{b0j}(1/P_j^2)\ . \tag{A23b}$$

The corresponding PP amplitudes can simply be obtained by replacing a,b by PP and R_j by $-R_j$. The rescaled width $G_{H_i}=\Gamma_{H_i}m_{H_i}/m_\chi^2$ as before, and the trilinear Higgs couplings are [42]

$$g_{111}=-\frac{3}{2\cos\theta_W}\cos2\alpha\cos(\alpha+\beta)\ , \tag{A24a}$$

$$g_{222}=-\frac{3}{2\cos\theta_W}\cos2\alpha\sin(\alpha+\beta)\ , \tag{A24b}$$

$$g_{112}=g_{121}=\frac{1}{2\cos\theta_W}[2\sin2\alpha\cos(\alpha+\beta)+\sin(\alpha+\beta)\cos2\alpha]\ , \tag{A24c}$$

$$g_{122}=g_{221}=-\frac{1}{2\cos\theta_W}[2\sin2\alpha\sin(\alpha+\beta)-\cos(\alpha+\beta)\cos2\alpha]\ , \tag{A24d}$$

$$g_{PP1}=g_{1PP}=\frac{\cos(\alpha+\beta)}{2\cos\theta_W}\cos2\beta\ , \tag{A24e}$$

$$g_{PP2}=g_{2PP}=-\frac{\sin(\alpha+\beta)}{2\cos\theta_W}\cos2\beta\ . \tag{A24f}$$

Recall that the suffix 1 (2) refers to the heavier (lighter) Higgs scalar.

7. $\chi\chi\to H_aP$

This process receives contributions from diagrams where one of the four neutralinos (labeled by j) is exchanged in the t or u channel, as well as from s-channel exchange of Z or P bosons. The result is

$A(^1S_0)$:

$$2\sqrt2g^2g_{aPP}T_{P00}\frac{R_Z}{4-R_P^2}\left[1+\frac{v^2}{8}\right]+\sqrt2g^2g_{aPZ}\frac{R_P^2-R_a^2}{R_Z^2}\left[1-\frac{v^2}{8}\right]-4\sqrt2g^2T_{a0j}T_{P0j}\frac{R_j}{P_j}\left[1+v^2\left[\frac18-\frac{1}{2P_j}+\frac{\bar\beta_f^2}{3P_j^2}\right]\right]-\sqrt2(R_P^2-R_a^2)g^2T_{a0j}T_{P0j}\left[1+v^2\left[-\frac18-\frac{1}{2P_j}+\frac{\bar\beta_f^2}{3P_j^2}\right]\right]; \tag{A25a}$$

$$A(^3P_1) : -4v\bar{\beta}_f \frac{g^2 g_{aPZ}}{4-R_Z^2+iG_Z} - 4v\bar{\beta}_f g^2 \frac{T_{a0i}T_{P0i}}{P_j} \ . \tag{A25b}$$

Here, $G_Z = M_Z\Gamma_Z/m_\chi^2$ as usual, and we have introduced the combinations of couplings

$$g_{1PZ} = -\frac{\sin(\alpha-\beta)}{2\cos^2\theta_W} O''^L_{00} \ , \tag{A26a}$$

$$g_{2PZ} = -\frac{\cos(\alpha-\beta)}{2\cos^2\theta_W} O''^L_{00} \ . \tag{A26b}$$

8. $\chi\chi \to H^+H^-$

This final state gets contributions from exchange of the two chargino states, labeled by j, as well as from the exchange of the Z boson and the two scalar Higgs bosons, labeled by i. The nonvanishing amplitudes are

$A(^3P_0)$:

$$-\sqrt{6}vg^2\left[(Q'^{L\,2}_{0j}+Q'^{R\,2}_{0j})\left(\frac{1}{P_j}-\frac{2\bar{\beta}_f^2}{3P_j^2}\right) + 2Q'^L_{0j}Q'^R_{0j}\frac{R_j^+}{P_j}\right] + \sqrt{6}vg^2R_W\frac{g_{+-i}}{4-R_{H_i}^2} \ ; \tag{A27a}$$

$A(^3P_1)$:

$$2v\bar{\beta}_f g^2(Q'^{L\,2}_{0j}-Q'^{R\,2}_{0j})\frac{1}{P_j} + 4v\bar{\beta}_f\frac{\cos 2\theta_W}{\cos^2\theta_W}g^2\frac{O''^L_{00}}{4-R_Z^2} \ ; \tag{A27b}$$

$A(^3P_2)$:

$$\frac{4}{\sqrt{3}}v\bar{\beta}_f^2 g^2(Q'^{L\,2}_{0j}+Q'^{R\,2}_{0j})\frac{1}{P_j^2} \ . \tag{A27c}$$

In Eqs. (A27) we have introduced the quantities

$$g_{+-1} = -T_{100}\left[\cos(\beta-\alpha) - \frac{\cos(\alpha+\beta)}{2\cos^2\theta_W}\cos 2\beta\right] , \tag{A28a}$$

$$g_{+-2} = -T_{200}\left[\sin(\beta-\alpha) + \frac{\sin(\alpha+\beta)}{2\cos^2\theta_W}\cos 2\beta\right] . \tag{A28b}$$

9. $\chi\chi \to f_a(h)\bar{f}_a(\bar{h})$

Here we use the suffices a,b to label the up and down components of weak isodoublets, with $T_{3,a} = \pm\frac{1}{2}$. This allows us to use the same notation for quarks and leptons. Of course, in the final cross section a color factor of 3 has to be included in case of quarks.

This final state can be produced by the exchange of the two sfermion eigenstates in the t and u channel, as well as by s-channel exchange of the Z boson or of one of the three neutral Higgs bosons. Since the final-state particles can be massless, we have to include finite widths for all s-channel propagators. We remind the reader that we do not expand s-channel propagators with respect to v, while we do expand t- and u-channel propagators. The contributing partial wave amplitudes can be written as

$A(^1S_0)$: $\lambda_f = 0$,

$$\sqrt{2}(-1)^{\bar{h}+1/2}(X'^2_{a0}+W'^2_{a0})\left[1+v^2\left[-\frac{1}{2P_1}+\frac{\bar{\beta}_f^2}{3P_1^2}\right]\right]\frac{R_f}{P_1}$$
$$+2\sqrt{2}(-1)^{\bar{h}+1/2}X'_{a0}W'_{a0}\frac{1}{P_1}\left[1+v^2\left[\frac{1}{4}-\frac{1}{2P_1}-\frac{\bar{\beta}_f^2}{6P_1}+\frac{\bar{\beta}_f^2}{3P_1^2}\right]\right]+(X'_{a0}\leftrightarrow Z'_{a0}, W'_{a0}\leftrightarrow Y'_{a0}, P_1\leftrightarrow P_2)$$
$$+(-1)^{\bar{h}+1/2}\frac{2\sqrt{2}g^2}{\cos^2\theta_W}O''^L_{00}T_{3a}\frac{R_f}{R_Z^2}+4\sqrt{2}(-1)^{\bar{h}+1/2}gh_{Pa}T_{P00}\frac{1}{4-R_P^2+iG_P}\left[1+\frac{v^2}{4}\right] \ ; \tag{A29a}$$

$A(^3P_0)$: $\lambda_f = 0$,

$$-\sqrt{6}v\bar{\beta}_f(X'_{a0}W'_{a0})\left[\frac{1}{P_1}-\frac{2}{3P_1^2}\right]+\sqrt{6}v\bar{\beta}_f(X'^2_{a0}+W'^2_{a0})\frac{R_f}{P_1^2}+(X'_{a0}\leftrightarrow Z'_{a0}, W'_{a0}\leftrightarrow Y'_{a0}, P_1\leftrightarrow P_2)$$
$$-2\sqrt{6}v\bar{\beta}_f g\frac{h_{ia}T_{i00}}{4-R_{H_i}^2+iG_{H_i}} \ ; \tag{A29b}$$

$A(^3P_1)$: $\lambda_f = 0$,

$$\frac{vR_f}{P_1}(X'^2_{a0}-W'^2_{a0})+(X'_{a0}\leftrightarrow Z'_{a0}, W'_{a0}\leftrightarrow Y'_{a0}, P_1\leftrightarrow P_2)-2g^2\frac{O''^L_{00}}{\cos^2\theta_W}\left[T_{3,a}-2e_{f_a}\sin^2\theta_W\right]\frac{R_f}{4-R_Z^2+iG_Z} \ ; \tag{A29c}$$

$\lambda_f=\pm 1$,

$$\sqrt{2}v\left[\lambda_f\bar{\beta}_f(X'^2_{a0}+W'^2_{a0})\left[-\frac{1}{P_1}+\frac{1}{P_1^2}\right]+(X'^2_{a0}-W'^2_{a0})\left[\frac{1}{P_1}-\frac{\bar{\beta}_f^2}{P_1^2}\right]+2\bar{\beta}_f\lambda_f(X'_{a0}W'_{a0})\frac{R_f}{P_1^2}\right]$$

$$+(X'_{a0}\leftrightarrow Z'_{a0},W'_{a0}\leftrightarrow Y'_{a0},P_1\leftrightarrow P_2)+2\sqrt{2}vg_Z^2O''^L_{00}[+\lambda_f T_{3,a}\bar{\beta}_f-(T_{3,a}-2e_{f_a}\sin^2\theta_W)]\frac{1}{4-R_Z^2+iG_Z}\ ; \tag{A29d}$$

$A(^3P_2)$: $\lambda_f=0$,

$$-\frac{2}{\sqrt{3}}v\bar{\beta}_f\frac{1}{P_1^2}[R_f(X'^2_{a0}+W'^2_{a0})+2X'_{a0}W'_{a0}]+(X'_{a0}\leftrightarrow Z'_{a0},W'_{a0}\leftrightarrow Y'_{a0},P_1\leftrightarrow P_2)\ ; \tag{A29e}$$

$\lambda_f=\pm 1$,

$$\sqrt{2}v\bar{\beta}_f\frac{1}{P_1^2}[-(X'^2_{a0}+W'^2_{a0})+\bar{\beta}_f\lambda_f(X'^2_{a0}-W'^2_{a0})-2R_fX'_{a0}W'_{a0}]+(X'_{a0}\leftrightarrow Z'_{a0},W'_{a0}\leftrightarrow Y'_{a0},P_1\leftrightarrow P_2)\ . \tag{A29f}$$

In Eqs. (A29), we have defined $R_f=m_{f_a}/m_\chi$ as in Eq. (A10c). These expressions fully include mixing between SU(2)-doublet and -singlet sfermions. The fermion mass eigenstates, labeled by 1 and 2 in Eqs. (A29), are defined by

$$\tilde{f}_1=\tilde{f}_L\cos\theta_f+\tilde{f}_R\sin\theta_f\ , \tag{A30a}$$

$$\tilde{f}_2=-\tilde{f}_L\sin\theta_f+\tilde{f}_R\cos\theta_f\ ; \tag{A30b}$$

the corresponding rescaled masses determine the inverse propagators P_1 and P_2 as shown in Eq. (A10b). Sfermion mixing also affects their couplings to neutralinos:

$$\begin{aligned}X'_{a0}&=X_{a0}\cos\theta_f+Z_{a0}\sin\theta_f\ ,\\ W'_{a0}&=Z_{a0}\cos\theta_f+Y_{a0}\sin\theta_f\ ,\\ Z'_{a0}&=-X_{a0}\sin\theta_f+Z_{a0}\cos\theta_f\ ,\\ Y'_{a0}&=-Z_{a0}\sin\theta_f+Y_{a0}\cos\theta_f\ .\end{aligned} \tag{A31}$$

The couplings of the unmixed sfermions in Eq. (A31) can be found in Ref. [42][16]:

$$X_{a0}=-\sqrt{2}g[T_{3a}N_{02}-\tan\theta_W(T_{3a}-e_{f_a})N_{01}]\ , \tag{A32a}$$

$$Y_{a0}=\sqrt{2}g\tan\theta_We_{f_a}N_{01}\ , \tag{A32b}$$

$$\begin{aligned}Z_{u0}&=-\frac{gm_u}{\sqrt{2}\sin\beta M_W}N_{04}\ ,\\ Z_{d0}&=-\frac{gm_d}{\sqrt{2}\cos\beta M_W}N_{03}\ .\end{aligned} \tag{A32c}$$

Finally, the couplings between Higgs bosons and SM fermions are [42]

$$h_{Pu}=-\frac{gm_u\cot\beta}{2M_W},\quad h_{Pd}=-\frac{gm_d\tan\beta}{2M_W}\ , \tag{A33a}$$

$$h_{1u}=-\frac{gm_u\sin\alpha}{2M_W\sin\beta},\quad h_{1d}=-\frac{gm_d\cos\alpha}{2M_W\cos\beta}\ , \tag{A33b}$$

$$h_{2u}=-\frac{gm_u\cos\alpha}{2M_W\sin\beta},\quad h_{2d}=\frac{gm_d\sin\alpha}{2M_W\cos\beta}\ . \tag{A33c}$$

[16]Notice that the last term in the relevant Eq. (5.5) of that reference has a wrong sign; Haber, private communication.

APPENDIX B: APPLICATION OF THE EQUIVALENCE THEOREM

As already discussed in Sec. II B, the high-energy limit of the amplitudes for the production of longitudinal gauge bosons can be understood from the equivalence theorem [50]. This also provides a useful check of these amplitudes. As an example, we discuss in this Appendix the production of two longitudinal Z bosons. We see from Eqs. (A15) that only two amplitudes contribute to the $\lambda=\bar{\lambda}=0$ final state; in the limit $|m_\chi|\gg M_Z$ they become

$$A(^3P_0)=-\frac{4\sqrt{6}g_Z^2v}{R_Z^2P_j}O''^{L\,2}_{0j}\left[\frac{2}{3}+R_j\left[1-\frac{2}{3P_j}\right]\right]$$

$$-\frac{2\sqrt{6}vg_2F_i}{(4-R_{H_i}^2)R_W}\ ; \tag{B1a}$$

$$A(^3P_2)=-\frac{8vg_Z^2}{\sqrt{3}R_Z^2P_j}O''^{L\,2}_{0j}\left[1+\frac{2R_j}{P_j}\right]\ , \tag{B1b}$$

where we have already made use of the fact that $O''^{L\,2}_{0j}\propto R_Z^2$, so that only contributions with an explicit factor $1/R_Z^2$ survive in the high-energy limit. More specifically, we see from Eqs. (6) that only the contributions from the Higgsino-like neutralinos ($j=3,4$) will survive in this limit:

$$R_3=-R_4=\mu/M_1\ ; \tag{B2a}$$

$$P_3=P_4=1+\mu^2/M_1^2\ ; \tag{B2b}$$

$$O''^{L\,2}_{03}+O''^{L\,2}_{04}=\frac{1}{4}\left[\frac{M_Z\sin\theta_W}{M_1^2-\mu^2}\right]^2$$

$$\times(M_1^2+\mu^2+2M_1\mu\sin 2\beta)\ ; \tag{B2c}$$

$$O''^{L\,2}_{03} - O''^{L\,2}_{04} = -\frac{1}{4}\left[\frac{M_Z \sin\theta_W}{M_1^2-\mu^2}\right]^2 \times[(M_1^2+\mu^2)\sin 2\beta + 2M_1\mu] \ . \quad \text{(B2d)}$$

In SUGRA, $m_\chi^2 \gg M_Z^2$ almost always implies $m_P^2 \gg M_Z^2$. In that case F_1 becomes very small, so that the contribution from the heavy Higgs scalar can be neglected; moreover, one has $R_{H_2}^2 \ll 1$ in this limit, and $\alpha = \beta + \pi/2$. This gives

$$F_2 = -T_{200} = \frac{M_Z \sin^2\theta_W}{\cos\theta_W(\mu^2-M_1^2)}(M_1 + \mu \sin 2\beta) \ , \quad \text{(B3)}$$

where we have used Eq. (6a). Inserting Eqs. (B2) and (B3) into (B1) finally yields

$$A(^3P_0) = -\sqrt{6}vg'^2 \frac{M_1^2}{\mu^2+M_1^2}\frac{1}{(\mu^2-M_1^2)^2}\left[\frac{2}{3}M_1^2(M_1^2+\mu^2+2M_1\mu\sin 2\beta) - M_1\mu\left[1-\frac{2}{3}\frac{M_1^2}{M_1^2+\mu^2}\right][(M_1^2+\mu^2)\sin 2\beta + 2M_1\mu]\right] - \frac{\sqrt{6}}{2}g'^2 v\frac{M_1}{\mu^2-M_1^2}(M_1+\mu\sin 2\beta) \ ; \quad \text{(B4a)}$$

$$A(^3P_2) = -\frac{2}{\sqrt{3}}vg'^2\frac{1}{M_1^2+\mu^2}\left[\frac{M_1^2}{M_1^2-\mu^2}\right]^2\left[M_1^2+\mu^2+2M_1\mu\sin 2\beta - \frac{2\mu M_1}{M_1^2+\mu^2}[(M_1^2+\mu^2)\sin 2\beta + 2M_1\mu]\right] \ . \quad \text{(B4b)}$$

The last term in Eq. (B4a) comes from Higgs exchange. One recognizes the form of our "symbolic" expression (13) of Sec. II B.

On the other hand, since the neutral Goldstone boson G is a pseudoscalar, the amplitudes for the production of a GG pair can be directly read off from our results for PP production, Eqs. (A23). Retaining only those terms that remain finite as $m_\chi^2/M_Z^2 \to \infty$, one has

$$A(^3P_0) = -\frac{2\sqrt{6}vg^2}{P_j}T_{G0j}^2\left[1-R_j-\frac{2}{3P_j}\right] \ , \quad \text{(B5a)}$$

$$A(^3P_2) = -\frac{8}{\sqrt{3}}vg^2 T_{G0j}^2\frac{1}{P_j^2} \ . \quad \text{(B5b)}$$

The couplings T_{G0j} can be obtained from Eq. (A9a) by the substitution $\sin\beta \to -\cos\beta$, $\cos\beta \to \sin\beta$. We see that again only the contributions from the exchange of the Higgsino-like neutralinos ($j=3,4$) survive:

$$T_{G03}^2 + T_{G04}^2 = \tfrac{1}{4}\tan^2\theta_W \ ; \quad \text{(B6a)}$$

$$T_{G03}^2 - T_{G04}^2 = -\frac{1}{4}\tan^2\theta_W \sin 2\beta \ . \quad \text{(B6b)}$$

Inserting this into Eqs. (A38) gives

$$A(^3P_0) = -\frac{\sqrt{6}}{2}vg'^2\frac{M_1^2}{M_1^2+\mu^2}\left[1-\frac{2}{3}\frac{M_1^2}{M_1^2+\mu^2}+\frac{\mu}{M_1}\sin 2\beta\right] \ ; \quad \text{(B7a)}$$

$$A(^3P_2) = -\frac{2}{\sqrt{3}}vg'^2\left[\frac{M_1^2}{M_1^2+\mu^2}\right]^2 \ . \quad \text{(B7b)}$$

While perhaps not immediately obvious, it can be shown that Eqs. (A40) are indeed identical to Eqs. (B4).

The fact that the Goldstone amplitudes (A40) automatically yield more compact expressions shows that they can not only be used to check some amplitudes of Appendix A, but they also allow to derive the high-energy limit of the amplitudes for the production of longitudinal gauge bosons more quickly. We saw already that the amplitudes for the production of transverse gauge bosons vanish with some power of M_Z/m_χ in the limit of large $|m_\chi|$ if X is b-ino-like; the longitudinal helicity states therefore dominate the total production of gauge bosons in this important special case. (This is not true for Higgsino-like or mixed LSP, however.) Most amplitudes for the production of Goldstone bosons can be read off directly from our results for the production of pseudoscalar and charged Higgs bosons, replacing $\sin\beta \to -\cos\beta$, $\cos\beta \to \sin\beta$ in the corresponding couplings of Higgs bosons to neutralinos and charginos. The only exception is H^+G^- production, which gives the high-energy limit of $H^+W_L^-$ production. We list the nonvanishing partial wave amplitudes for completeness:

$$^1S_0:\ 2\sqrt{2}g^2Q'^L_{0j}Q'^R_{0j}\frac{R_j^+}{1+R_j^{+2}}\left[1+v^2\left[\frac{1}{8}-\frac{1}{2(1+R_j^{+2})}+\frac{1}{3(1+R_j^{+2})^2}\right]\right]; \tag{B8a}$$

$$^3P_0:\ -\frac{\sqrt{6}}{2}v\sin 2\beta g^2(Q'^{L^2}_{0j}-Q'^{R^2}_{0j})\left[\frac{1}{1+R_j^{+2}}-\frac{2}{3(1+R_j^{+2})^2}\right]+\sqrt{6}vg^2Q'^L_{0j}Q'^R_{0j}\cos 2\beta\frac{R_j^+}{1+R_j^{+2}}; \tag{B8b}$$

$$^3P_1:\ v\sin 2\beta g^2(Q'^{L^2}_{ij}+Q'^{R^2}_{ij})\frac{1}{1+R_j^{+2}}; \tag{B8c}$$

$$^3P_2:\ -\frac{2}{\sqrt{3}}v\sin 2\beta g^2\frac{Q'^{L^2}_{0j}-Q'^{R^2}_{0j}}{(1+R_j^{+2})^2}. \tag{B8d}$$

In Eqs. (B8), we have again only kept terms that remain finite at high energies.

[1] See, e.g., *Proceedings of the ESO-CERN Topical Workshop on LEP and the Early Universe,* edited by J. Ellis, P. Salati, and P. Shaver (CERN Report No. TH.5709/90, Geneva, Switzerland, in press).

[2] For a review, see S. K. Blau and A. Guth, in *300 Years of Gravitation,* edited by S. Hawking and W. Israel (Cambridge University Press, Cambridge, England, 1987).

[3] P. J. E. Peebles, D. N. Schramm, E. L. Turner, and R. G. Kron, Nature **352**, 769 (1991).

[4] E. W. Kolb and M. S. Turner, *The Early Universe* (Addison-Wesley, New York, 1990).

[5] H. Goldberg, Phys. Rev. Lett. **50**, 1419 (1983); J. Ellis, J. Hagelin, D. V. Nanopoulos, and M. Srednicki, Phys. Lett. **127B**, 233 (1983).

[6] For a review of the MSSM, see H. E. Haber and G. L. Kane, Phys. Rep. **117**, 75 (1985).

[7] For reviews of phenomenological supergravity, see H. P. Nilles, Phys. Rep. **110**, 1 (1984); P. Nath, R. Arnowitt, and A. Chamseddine, *Applied N=1 Supergravity* (World Scientific, Singapore, 1984).

[8] E. Witten, Nucl. Phys. **B188**, 513 (1981); N. Sakai, Z. Phys. C **11**, 153 (1981); S. Dimopoulos and H. Georgi, Nucl. Phys. **B193**, 150 (1981).

[9] E. Gildener and S. Weinberg, Phys. Rev. D **13**, 3333 (1976); E. Gildener, *ibid.* **14**, 1667 (1976).

[10] K. Inoue, A. Kakuto, H. Komatsu, and S. Takeshita, Prog. Theor. Phys. **68**, 927 (1982); **71**, 413 (1984); L. E. Ibáñez and G. G. Ross, Phys. Lett. **110B**, 215 (1982); L. E. Ibáñez, *ibid.* **118B**, 73 (1982); J. Ellis, D. V. Nanopoulos, and K. Tamvakis, *ibid.* **121B**, 123 (1983); L. Alvarez-Gaumé, J. Polchinski, and M. B. Wise, Nucl. Phys. **B221**, 495 (1983).

[11] S. Bertolini, F. Borzumati, A. Masiero, and G. Ridolfi, Nucl. Phys. **B353**, 591 (1991), and references therein.

[12] M. Drees, K. Hagiwara, and A. Yamada, Phys. Rev. D **45**, 1725 (1992).

[13] LEP Collaborations, Phys. Lett. B **276**, 247 (1992).

[14] U. Amaldi, W. de Boer, and H. Fürstenau, Phys. Lett. B **260**, 447 (1991); P. Langacker and M. Luo, Phys. Rev. D **44**, 817 (1991); J. Ellis, S. Kelley, and D. V. Nanopoulos, Phys. Lett. B **260**, 131 (1991).

[15] J. Ellis, S. Kelley, and D. V. Nanopoulos, Nucl. Phys. **B373**, 55 (1992).

[16] G. G. Ross and R. G. Roberts, Nucl. Phys. **B377**, 571 (1992).

[17] J. Ellis, J. Hagelin, D. V. Nanopoulos, K. Olive, and M. Srednicki, Nucl. Phys. **B238**, 453 (1984); K. Griest, Phys. Rev. D **38**, 2357 (1988).

[18] K. Griest, M. Kamionkowski, and M. S. Turner, Phys. Rev. D **41**, 3565 (1990).

[19] K. Olive and M. Srednicki, Phys. Lett. B **230**, 78 (1989); Nucl. Phys. **B355**, 208 (1991).

[20] J. L. Lopez, D. V. Nanopoulos, and K. Yuan, Nucl. Phys. **B370**, 445 (1992).

[21] J. Ellis, J. Hagelin, and D. V. Nanopoulos, Phys. Lett. **159B**, 26 (1985).

[22] M. M. Noriji, Phys. Lett. B **261**, 76 (1991).

[23] J. L. Lopez, D. V. Nanopoulos, and K. Yuan, Phys. Lett. B **267**, 219 (1991).

[24] J. Ellis and L. Roszkowski, Phys. Lett. B **283**, 252 (1992).

[25] S. Kelley, J. L. Lopez, D. V. Nanopoulos, H. Pois, and K. Yuan, Phys. Lett. B **273**, 423 (1991).

[26] J. MacDonald, K. A. Olive, and M. Srednicki, Phys. Lett. B **283**, 80 (1992).

[27] J. Ellis and F. Zwirner, Nucl. Phys. **B338**, 317 (1990).

[28] For a review, see A. B. Lahanas and D. V. Nanopoulos, Phys. Rep. **145**, 1 (1987).

[29] J. Ellis, L. Roszkowski, and Z. Lalak, Phys. Lett. B **245**, 545 (1990).

[30] Y. Okada, M. Yamaguchi, and T. Yanagida, Prog. Theor. Phys. **85**, 1 (1991); Phys. Lett. B **262**, 54 (1991); H. E. Haber and R. Hempfling, Phys. Rev. Lett. **66**, 1815 (1991); J. Ellis, G. Ridolfi, and F. Zwirner, Phys. Lett. B **257**, 83 (1991); **262**, 477 (1991); R. Barbieri, M. Frigeni, and F. Caravaglio, *ibid.* **258**, 395 (1991).

[31] G. F. Giudice and G. Ridolfi, Z. Phys. C **41**, 447 (1988); M. Olechowski and S. Pokorski, Phys. Lett. B **214**, 239 (1988); W. Majerotto and B. Mösslacher, Z. Phys. C **48**, 273 (1990).

[32] M. Drees and M. M. Nojiri, Nucl. Phys. **B369**, 54 (1992).

[33] L. Roszkowski, Phys. Lett. B **262**, 59 (1991).

[34] L. Roszkowski, Phys. Lett. B **278**, 147 (1992).

[35] R. Barbieri and G. F. Giudice, Nucl. Phys. **B306**, 63 (1988).

[36] M. Srednicki, R. Watkins, and K. A. Olive, Nucl. Phys. **B310**, 693 (1988).

[37] K. Griest and D. Seckel, Phys. Rev. D **43**, 3191 (1991).

[38] J. Ellis, D. V. Nanopoulos, L. Roszkowski, and D. N. Schramm, Phys. Lett. B **245**, 251 (1990); L. Krauss, Phys. Rev. Lett. **64**, 999 (1990).

[39] S. Wolfram, Phys. Lett. **82B**, 65 (1979); C. B. Dover, T. K. Gaisser, and G. Steigman, Phys. Rev. Lett. **42**, 1117 (1979). For experimental bounds on charged stable relics, see P. F. Smith *et al.*, Nucl. Phys. **B206**, 333 (1982).
[40] H. Baer, M. Drees, and X. Tata, Phys. Rev. D **41**, 3414 (1990).
[41] D. Caldwell *et al.*, Phys. Rev. Lett. **61**, 510 (1988).
[42] J. F. Gunion and H. E. Haber, Nucl. Phys. **B272**, 1 (1986).
[43] M. Drees, C. S. Kim, and X. Tata, Phys. Rev. D **37**, 784 (1987).
[44] A. Bartl, H. Fraas, W. Majerotto, and N. Oshimo, Phys. Rev. D **40**, 1594 (1989); M. Guchait, Jadavpur University (Calcutta) Report No. 92-0052 (unpublished).
[45] For a recent review, see M. Davier, in *Proceedings of the Joint International Lepton-Photon Symposium and Europhysics Conference on High Energy Physics,* Geneva, Switzerland, 1991, edited by S. Hegarty, K. Potter, and E. Quercigh (World Scientific, Singapore, 1992); Orsay Report No. LAL 91-48 (unpublished).
[46] L. Pondrom, in *Proceedings of the 25th International Conference on High Energy Physics,* Singapore, 1990, edited by K. K. Phua and Y. Yamaguchi (World Scientific, Singapore, 1991).
[47] H. Baer, X. R. Tata, and J. Woodside, Phys. Rev. D **44**, 207 (1991).
[48] L. Roszkowski, Phys. Lett. B **252**, 471 (1990); K. Hidaka, Phys. Rev. D **44**, 927 (1991).
[49] J. Ellis and S. Rudaz, Phys. Lett. **128B**, 248 (1983).
[50] B. W. Lee, C. Quigg, and H. Thacker, Phys. Rev. D **16**, 1519 (1977); M. S. Chanowitz and M. K. Gaillard, Nucl. Phys. **B261**, 379 (1985). For a rigorous proof, see H. Veltman, Phys. Rev. D **41**, 2294 (1990).
[51] L. E. Ibáñez and C. Lopez, Nucl. Phys. **B233**, 511 (1984); A. Kounnas, A. B. Lahanas, D. V. Nanopoulos, and M. Quirós, *ibid.* **B236**, 438 (1984); A. Bouquet, J. Kaplan, and C. A. Savoy, *ibid.* **B262**, 299 (1985).
[52] M. Drees and M. M. Nojiri, Phys. Rev. D **45**, 2482 (1992).
[53] G. Gamberini, G. Ridolfi, and F. Zwirner, Nucl. Phys. **B331**, 331 (1990).
[54] K. Inoue, A. Kakuto, H. Komatsu, and S. Takeshita, Prog. Theor. Phys. **67**, 1889 (1982); R. A. Flores and M. Sher, Ann. Phys. (N.Y.) **148**, 95 (1983).
[55] Some recent papers on supersymmetry breaking in superstring theories are M. K. Gaillard, A. Papadopoulos, and D. M. Pierce, Phys. Rev. D **45**, 2057 (1992); L. E. Ibáñez and D. Lüst, Nucl. Phys. **B382**, 305 (1992).
[56] ALEPH Collaboration, D. Decamp *et al.*, Phys. Rep. **216**, 253 (1992).
[57] J. M. Frère, D. R. T. Jones, and S. Raby, Nucl. Phys. **B222**, 11 (1983); M. Claudson, L. Hall, and I. Hinchliffe, *ibid.* **B228**, 501 (1983).
[58] P. Nath, A. H. Chamseddine, and R. Arnowitt, Phys. Rev. D **32**, 2348 (1985); R. Arnowitt and P. Nath, Phys. Rev. Lett. **69**, 725 (1992).
[59] CDF Collaboration, F. Abe *et al.*, Phys. Rev. D **45**, 3921 (1992).
[60] J. Grivaz, in *Proceedings of the Workshop on Physics and Experiments with Linear Colliders,* Saariselkä, Finland, 1991, edited by R. Orava, P. Eerola, and M. Nordberg (World Scientific, Singapore, in press).
[61] For a review, see D. O. Caldwell, lectures given at the International School on Astroparticle Physics, The Woodlands, Texas, 1991, University of California (Santa Barbara) Report No. UCSB-HEP-91-04 (unpublished).
[62] F. Halzen, T. Stelzer, and M. Kamionkowski, Phys. Rev. D **45**, 4439 (1992).
[63] V. Barger, E. W. N. Glover, K. Hikasa, W. Y. Keung, M. G. Olsson, C. J. Suchyta, and X. R. Tata, Phys. Rev. D **35**, 3366 (1987).